Close-Form Design of Antenna-Constrained Multi-Cell Multi-User Downlink Interference Alignment

Haichuan Zhou, Tharm Ratnarajah†
The Institute of Electronics, Communications and Information Technology (ECIT),
Queen's University Belfast, Queen's Road, Belfast, UK
†The University of Edinburgh, Edinburgh, UK
Email: hzhou01@qub.ac.uk

Abstract

This paper investigates the downlink channels in multi-cell multi-user interfering networks. The goal is to propose close-form designs to obtain degrees of freedom (DoF) in high SNR region for the network composed of base stations (BS) as transmitters and mobile stations (MS) as receivers. Consider the realistic system, both BS and MS have finite antennas, so that the design of interference alignment is highly constrained by the feasibility conditions. The focus of design is to explore potential opportunities of alignment in the subspace both from the BS transmit side and from the MS receive side. The new IA schemes for cellular downlink channels are in the form of causal dynamic processes in contrary to conventional static IA schemes. For different implementations, system conditions are compared from all aspects, which include antenna usage, CSI overhead and computational complexity. This research scope covers a wide range of typical multi-cell multi-user network models. The first one is a K-cell fully connected cellular network; the second one is a Wyner cyclic cellular network with two adjacent interfering links; the third one is a Wyner cyclic cellular network with single adjacent interfering link considering cell-edge and cell-interior users respectively.

I. Introduction

Cellular networks have been intensively studied for years from all kinds of theoretical models to various complicated realistic settings. The single cell model has been investigated in the prevalent scenario of multi-user MIMO (MU-MIMO) networks [1], [2], [3]. In MU-MIMO, the base stations (BS) simultaneously transmit to multiple receivers, i.e. mobile stations (MS), which form a typical MIMO broadcast downlink channel. The self-interferences among multiple streams cause performance degradation for each MS. While with perfect channel state information both at the transmitters (CSIT) and at the receivers (CSIR), capacity could be achieved by using Gaussian codes, linear beamforming as well as dirty-paper-coding (DPC). Since DPC is hard to implement, opportunistic beamforming combined with user selection could also asymptotically approach the gain. The maximum number of degrees of freedom (DoF) in MU-MIMO is $\min(N_t, KN_r)$, where N_t is the number of BS transmit antennas, K is the number of MS users, and N_r is the number of MS receive antennas. Recently, the model of multi-cell network also receives a rich body of research [4], [5], [6]. Its downlink scenario is coined as the interfering broadcast channel (IFBC or IBC), while the uplink channel is called the interfering multiple access (IMAC) channel. From a practical perspective, the multi-cell and multi-user downlink transmission schemes have been actively discussed for fourth-generation (4G) cellular systems such as network MIMO and coordinated multi-point communication (CoMP) in the interference-limited environment [7]. In particular, systems such as LTE-Advanced as well as IEEE802.16m require a great increase in cell-edge spectral efficiency over previous 3G systems [8], [9]. Interferences between cells and users are the key bottleneck for the whole network to boost system capacity, so that a common goal of these schemes is to effectively mitigate interferences. Thus interference management techniques are intensively investigated to improving cell-edge throughput [4]. It was shown that near interference-free throughput performance can be achieved in the cellular network [10]. In our following work, only downlink channels are considered, and all the parts focus on the model of IFBC channels.

A. Multi-Cell Downlink Interference Alignment Methods

Interference management based on multi-cell cooperation can dramatically improve the system performance. The recently emerging technique of interference alignment (IA) is a promising interference management scheme to mitigate interferences in term of DoF in high SNR region. However, since all the scenarios and schemes only consider time-invariant/constant channels regarding practical requirements, there are finite spatial signal dimensions created by multiple antennas on each node without any frequency or time extensions. Then it is hard to achieve interference alignment with only finite dimensions either by using numerical algorithms or analytical designs.

Regarding the methods of iterative algorithms, there are not many results from initial studies. [11] explicitly explores the feasibility condition of linear interference alignment in constant MIMO cellular networks. [12], [13] extend the iterative interference alignment algorithm in interference channels to IFBC channels, but the alignment is implicit and requires a large amount of iterations. [5] looks into a special clustered shifting approach.

Regarding the methods of analytical designs, there are in general three significant approaches. The first approach is in [14], [10] where two cascaded precoders are set for each transmitter (BS) node. The preceding precoder is designed to represent

inter-cell interference (ICI) subspace with respect to other users, while the subsequent precoder is designed to represent inter-user interference (IUI) subspace. Because they are cascaded, the IUI subspace is contained in the ICI subspace, i.e. aligned. This scheme is only for a two-cell network. The second approach is in [15], [16], [17] where a predetermined reference subspace is set for every user receiver to align the interference coming from the other BSs. Thus all the effective subspaces generated from one BS interfering with receivers in the other cell are aligned and orthogonal to the desired signal subspace, which is a duality design process compared with [14], [10]. No back-and-forth signalling is needed between the BS side and MS side. The third approach is in [18] where an intricate and meticulous DoF design is realized in a two-cell and two-user per cell MIMO IFBC channel. By a novel jointly design of transmit and receive beamforming vectors in a closed-form expression without any iterative computation, it outperforms previous method in [14], [10] and [19], [20] in terms of antenna usage and DoF. The process includes two main steps. The receive beamforming vectors first align effective inter-cell interferences, and then the transmit beamforming vectors remove both inter-cell interferences and inter-user interferences.

B. Multi-Cell Downlink Interference Alignment Issues

It is absolutely challenging to design general interference alignment schemes for multi-cell downlink channels. Broadly speaking, there are three key issues worthy attention:

First, the above three existing approaches of [14], [15] and [18] mainly consider the configuration of two cells with two users in each cell as well as single data stream for each user. It is highly non-trivial to extend the case to a general scenario in which more than two cells, more than two users in each cell, and multiple data streams are involved in the network. So the new scenario is distinct from either the original IA problem in the K-pair interference channel [21] or the two-user cellular channel [18], [14]. In brief, the multi-cell network has more complicated interfering structures to proceed alignment. For each user in each cell, it receives interferences from: multiple streams of its own; interfering streams from other intra-cell users; multiple interfering links from BSs in other cells. Accordingly various levels of alignment are necessary for different sources of interferences.

Second, multiple antenna (MIMO) configuration is becoming a critical issue in term of DoF obtainable by IA. Conventional research works usually adopt finite transmit antennas and single receive antenna, e.g. MU-MIMO, so that it only needs to design the transmit beamforming vectors to remove IUI. However, multiple antennas are nowadays introduced at the mobile stations in the 3GPP LTE, IEEE 802.16e systems [8], [9]. For example, the configuration of 4 transmit antennas and 4 receive antennas is one option of antennas in the 4G standards. Hence a lot of recent works take multiple receive antennas as well as transmitter antennas into account in the coordinated scheme for MIMO IFBC channels. [14] and [22] assume sufficient number of transmitter antennas so that explicit IA conditions are guaranteed to achieve; [15], [16], [17] particularly rely on multiple receive antennas to construct the predefined interference subspace; [18] delicately confines a critical range of the number of transmit antennas N_t and the number of receive antennas N_r, satisfying $3N_r/2 < N_t < 2N_r$. The range of transmit and receive antennas reflects a very subtle balance that both transmit side and receive side are capable of contributing to the construction of IA via a precise and dedicated cooperation, although it needs large overhead of CSI exchange between BSs and MSs in the cells.

Third, as just mentioned, the transmitters require perfect channel state information (CSI) specified as CSIT, and receivers may also require channel CSI as CSIR. The huge amount of coordinations between nodes are supported by all the CSI so that IA schemes are implemented in realistic cellular networks. To acquire CSI, a relatively modest amount of backhaul communication is needed [4]; training and feedback are also carried out within the cell and across cells [23]. However, as CSI requirements increase, the corresponding system overhead may cause bottleneck that limits the growth of dimensionality and spectral efficiency.

C. Aims and Contributions of This Work

Regarding the mentioned scenarios, methods and issues, the aims and contributions of this work could be summarized into the following aspects:

1) An explicit close-form structure is built for interference alignment in general multi-cell (more than two cells) networks. The IA structure is constructed in a standardized dynamic procedure, where different parts in the interfering structure interplay with each other step by step and alignments are made in diverse levels.

2) Three types of models of multi-cell networks are analyzed respectively. One is an ordinary full connected symmetric network, which has K cells, M users per cell, and d streams per user. The other is a cyclic symmetric Wyner-type network [24], in which the MSs in each cell suffer interferences only from BSs in two adjacent cells. The last is a cyclic asymmetric Wyner-type network, also known as the cascaded Z-interference channel [25]. In this network, MSs in each cell suffer interferences only from the BS in one adjacent cell, and moreover the distinction between cell-interior MSs and cell-edge MSs is considered.

3) Both transmit side and receive side are involved and balanced to satisfy zero-forcing conditions for IA. Regarding finite antennas, CSI overhead and computational complexity, three options are provided for IA design: only on the transmit side; only on the receive side; tradeoff of two sides.

4) Cascaded precoders or receive filters could simplify cooperations between nodes, however they consume a number of antennas for every node. So this work looks into the balance between the complicacy of cascaded coders and antenna numbers as well as CSI overhead and computational complexity. Meanwhile the performance loss due to residue interference of imperfect alignment is also evaluated.

5) Due to concerns of the implementation of practical systems, a robust measure of coder selection method is also provided. Conventional schemes adopt fixed random precoders in [14] on the transmit side and identical predetermined filters in [15] on the receive side. Therefore, the system performance could be improved by selecting appropriate coders as in [26], [27], [28]. For example, on the transmit side, the fixed random precoder matrix is set to be finitely optional to be aligned. The solution is robust and the antenna usage could be saved to some extent.

6) Instead of static structure designs in conventional IA schemes, dynamic procedures are introduced due to the complicacy of the network. High DoF are reachable from the direct interplay between interfering cells. Alignments are arranged in a natural way between the transmit side and the receive side.

The following parts are organized as: Section II introduces and describes all the scenarios and models; Section III designs and analyzes the full connected network; Section IV discusses the Wyner-type network with two adjacent interfering links; Section V discusses the Wyner-type network with one adjacent interfering link; Section VI proposes advanced designs for the Wyner-type networks; Section VII gives a summary and conclusion.

II. Problem Statement and Model Description

Before the discussion of the three models of cellular networks in this work, common settings are described for all these scenarios. The network contains K cells. Each cell has one base stations (BS), and M users, i.e. mobile stations (MS). The BSs are denoted in a set as $\mathcal{K} = \{1, 2, \ldots, K\}$ and the MSs in an individual cell are denoted in a set as $\mathcal{M} = \{1, 2, \ldots, M\}$. Each BS is equipped with N_t antennas and each MS is equipped with N_r antennas. Denote $\mathbf{H}_{k'}^{k:m} \in \mathbb{C}^{N_r \times N_t}$ as the channel from k'-th BS to to m-th MS in the k-th cell. d is the number of datastreams from arbitrary k-th BS to m-th MS in its own cell. So that define $\mathbf{V}_{k:m} \in \mathbb{C}^{N_t \times d}$ as the precoder at k-th BS for the m-th MS in its own cell, and define $\mathbf{x}_{k:m} \in \mathbb{C}^{d \times 1}$ as the corresponding input streams at BS. Similarly, define $\mathbf{U}_{k:m} \in \mathbb{C}^{N_r \times d}$, $\mathbf{y}_{k:m} \in \mathbb{C}^{N_r \times 1}$ and $\hat{\mathbf{y}}_{k:m} = \mathbf{U}_{k:m}^{\dagger}\mathbf{y}_{k:m} \in \mathbb{C}^{d \times 1}$ as the receive filter, received signal and output streams at m-th MS in k-th cell.

Notice: since all discussions are regarding DoF design in high SNR region, the noise terms are ignored in following expressions.

A. Model 1: Full Connected Network

Model 1 is shown as in Fig. 1, which is a symmetric full connected network with K cells interfering to each other. For simplicity of expressions, a special model of three cells with three users in each cell is used for illustration. However, all the schemes and results shown could be directly applied to K-cell networks with losing generality. Compared with the conventional scenario of two cells in the network as in [18], [14], [15], the three-cell scenario is intrinsically different and complicated, because MSs in each cell observe more than two interfering cells which have a potential to cooperate.

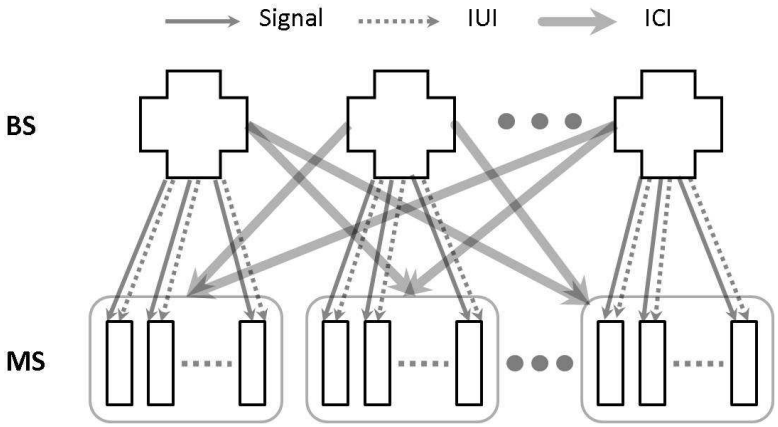

Fig. 1. Model 1: Full Connected Network

The received signal at m-th MS of k-th cell is shown in equation (1):

$$\begin{aligned}\mathbf{y}_{k:m} = \mathbf{H}_k^{k:m}\mathbf{V}_{k:m}\mathbf{x}_{k:m} + \sum_{n\neq m}^{n\in\mathcal{M}} \mathbf{H}_k^{k:m}\mathbf{V}_{k:n}\mathbf{x}_{k:n} \\ + \sum_{j\neq k}^{j\in\mathcal{K}} \sum_{n\in\mathcal{M}} \mathbf{H}_j^{k:m}\mathbf{V}_{j:n}\mathbf{x}_{j:n}\end{aligned} \tag{1}$$

While the received signal $\mathbf{y}_{k:m}$ in (1) is composed of three parts: desired signal, intra-cell interference (IUI) from users in the same cell, and inter-cell interference (ICI) from all other cells.

B. Model 2: Cyclic Network with Two-Side Adjacent Links

Model 2 is shown as in Fig. 2, which is a cyclic network with users in each cell only interfered by two adjacent cells. It is a simple and tractable model proposed by Wyner [24]. The cells are arranged in an infinite linear array or equivalently on a circle [29] , [30].

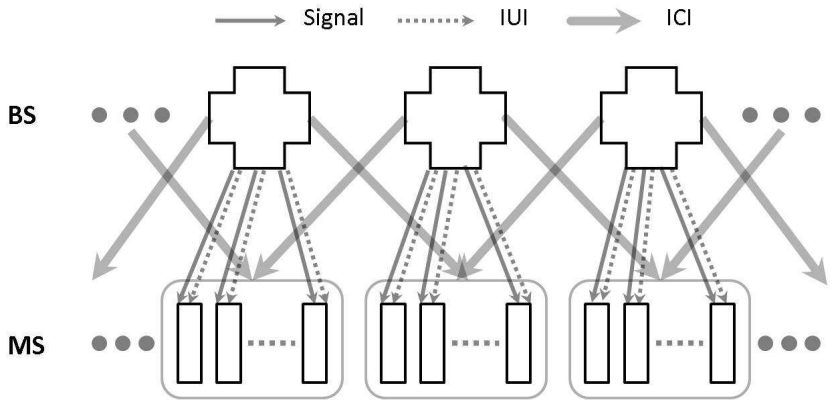

Fig. 2. Model 2: Cyclic Network with Two-Side Adjacent Links

The received signal at m-th MS of k-th cell is shown in equation (2):

$$\begin{aligned}\mathbf{y}_{k:m} = \mathbf{H}_k^{k:m}\mathbf{V}_{k:m}\mathbf{x}_{k:m} + \sum_{n\neq m}^{n\in\mathcal{M}} \mathbf{H}_k^{k:m}\mathbf{V}_{k:n}\mathbf{x}_{k:n} \\ + \sum_{n\in\mathcal{M}} \mathbf{H}_{k-1}^{k:m}\mathbf{V}_{k-1:n}\mathbf{x}_{k-1:n} + \sum_{n\in\mathcal{M}} \mathbf{H}_{k+1}^{k:m}\mathbf{V}_{k+1:n}\mathbf{x}_{k+1:n}\end{aligned} \tag{2}$$

While the received signal $\mathbf{y}_{k:m}$ in (2) is composed of four parts: desired signal, intra-cell interferences (IUI) from users in the same cell, inter-cell interferences (ICI) from one adjacent cell on one side, and ICI from the other adjacent cell on the other side.

C. Model 3: Cyclic Network with One-Side Link only at Edge

Model 3 is shown in Fig. 3, which is a cyclic network where each cell has both cell-interior users and cell-edge users. Only the cell-edge users are interfered by only the adjacent cell on one side. It is motivated by the modified Wyner model as in [31], [30] and the cascaded Z-interference channel as in [25]. The different roles of cell-interior users and cell-edge users are also worth attention in practical systems [6].

Denote $\mathcal{M}^\star, \mathcal{M}^\circ \subset \mathcal{M}$ as the sets of cell-interior users and cell-edge users respectively. $|\mathcal{M}^\star| = M^\star$, $|\mathcal{M}^\circ| = M^\circ$ and $M^\star + M^\circ = M$. Each cell-interior MS has $N_r^\star$ antennas, while each cell-edge MS has N_r° antennas.

For cell-interior users, the received signal at $m^\star$-th ($m^\star \in \mathcal{M}^\star$) MS of k-th cell is shown in equation (3):

$$\begin{aligned}\mathbf{y}_{k:m^\star} = \mathbf{H}_k^{k:m^\star}\mathbf{V}_{k:m^\star}\mathbf{x}_{k:m^\star} + \sum_{n^\star\neq m^\star}^{n^\star\in\mathcal{M}^\star} \mathbf{H}_k^{k:m^\star}\mathbf{V}_{k:n^\star}\mathbf{x}_{k:n^\star} \\ + \sum_{n^\circ\in\mathcal{M}^\circ} \mathbf{H}_k^{k:m^\star}\mathbf{V}_{k:n^\circ}\mathbf{x}_{k:n^\circ}\end{aligned} \tag{3}$$

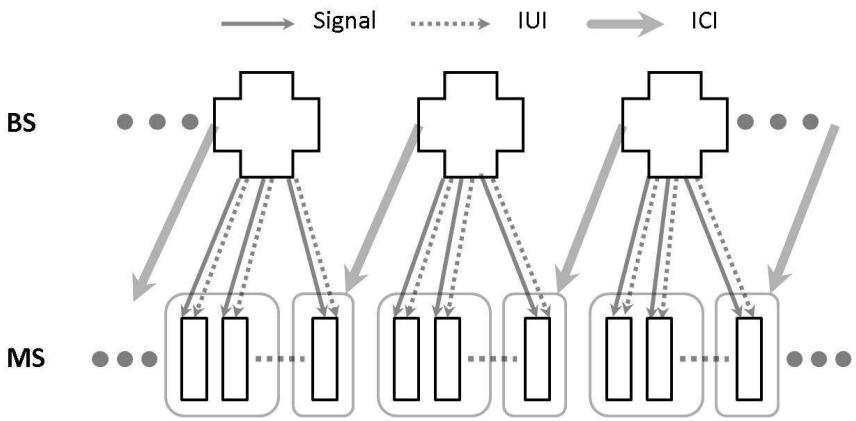

Fig. 3. Model 3: Cyclic Network with One-Side Link only at Edge

Then the received signal $\mathbf{y}_{k:m^\star}$ in (3) is composed of three parts: desired signal; IUI intended for other cell-interior users in the same cell; IUI intended for all cell-edge users in the same cell.

For cell-edge users, the received signal at m°-th ($m^\circ \in \mathcal{M}^\circ$) MS of k-th cell is shown in equation (4):

$$\begin{aligned}\mathbf{y}_{k:m^\circ} &= \mathbf{H}_k^{k:m^\circ}\mathbf{V}_{k:m^\circ}\mathbf{x}_{k:m^\circ} \\ &+ \sum_{n^\star\in\mathcal{M}^\star}\mathbf{H}_k^{k:m^\circ}\mathbf{V}_{k:n^\star}\mathbf{x}_{k:n^\star} + \sum_{n^\circ\neq m^\circ}^{n^\circ\in\mathcal{M}^\circ}\mathbf{H}_k^{k:m^\circ}\mathbf{V}_{k:n^\circ}\mathbf{x}_{k:n^\circ} \\ &+ \sum_{n^\star\in\mathcal{M}^\star}\mathbf{H}_{k+1}^{k:m^\circ}\mathbf{V}_{k+1:n^\star}\mathbf{x}_{k+1:n^\star} + \sum_{n^\circ\in\mathcal{M}^\circ}\mathbf{H}_{k+1}^{k:m^\circ}\mathbf{V}_{k+1:n^\circ}\mathbf{x}_{k+1:n^\circ}\end{aligned} \tag{4}$$

Then the received signal $\mathbf{y}_{k:m^\circ}$ in (4) is composed of five parts: desired signal; IUI intended for all cell-interior users in the same cell; IUI intended for other cell-edge users in the same cell; ICI from the adjacent cell intended for all its own cell-interior users; ICI from the adjacent cell intended for all its own cell-edge users.

D. Characteristics of Dealing with Multi-Cell Downlink IA

Since the models of multi-cell downlink channels are complicated to directly reach the status of interference alignment, the designs should be to generalized to be along three most critical threads. The three threads include interference decomposition, alignment planning, and process control, which are described as following.

1) Interference Decomposition: In the conventional K-pair peer-peer interference channel, all the interferences are seen at the same level symmetrically from equal sources to equal destinations. While in the downlink channels of cellular networks, all the interferences are distinguished to different levels according to their different sources and destinations. They are mainly categorized into three levels: from one BS to one MS in its own cell, the link has multiple streams which cause interferences between each other; from one BS to multiple MSs of its own cell, streams to one MS cause interferences to streams to another MS, which is defined as inter-user interference (IUI), i.e. with cross links overlapping the direct links [12]; from one BS to all MSs in another cell, all the streams (including desired signals, inter-stream interference and IUI in the cell) cause interferences to the other cell.

2) Alignment Planning: Since all the interference is decomposed into different levels and different parts, accordingly, it is necessary to make reasonable alignment, not simply overlapping all the interference. In principle, the more interferences are possibly aligned together, the less dimensionality of subspace they occupy, and the more DoF the network could obtain. In detail, it gives rise to complicated options to plan the alignment. Primarily, alignment are made at the same levels. Align inter-stream interference with inter-stream interference, IUI with IUI, ICI with ICI from one same cell. Secondarily, consider alignment between different levels of interferences. Usually, IUI could be aligned with ICI as shown in [14], [15], [18]; Third, notice this work is looking into the new scenario and model of multi-cell networks, so the new alignment between ICI and ICI from different cells are considered deliberately. Nevertheless, there also exist other potential options than the ones just mentioned.

3) Process Control: Even if the alignment planning is perfect made, the coding for all nodes are not possible to be determined and set in one time. All different levels and different sources of interferences are aligned step by step. A new issue worth attention is that alignment could be made either at the BS side or at the MS side, i.e. the transmitted signals are aligned or

the received signals are aligned. Another issue is the acquisition of CSI to satisfy the causality conditions between the steps of alignment. Profound cooperations are needed between BS and BS, MS and MS, intra-cell BS and MS, inter-cell BS and MS, etc. as in [29]. In particular, a *chicken-and-egg* problem arises in this whole process, because all the steps are related or coupled back and forth and here and there, between desired signals and interferences, BSs and MSs, intra-cell and inter-cell.

III. Basic Design and Analysis of Model 1

This section looks into model 1 as shown in Fig. 1 and equation (1). In general, there are three angles to implement the design. Recent works [14], [15], and [18] implement the alignment through reference subspace on the BS side, subspace on the MS side, and meticulous interplay on both BS and MS sides, respectively. According these three angles, the following work proposes five approaches to implement the alignment.

Clarification: Be advised that, in the following expressions of the design process, when a same BS or MS in a set is referred, the index may change between successive steps according to its subject or object position in the context of the current step. In each step, the index refers to all equal nodes. Specifically, k is used to denote the subject, and j is used to denote the object. Besides, in the corresponding tables, the index may also change according to the context of discussion.

Notations: with a little abuse, denote $\mathbf{A}^{-1}$ as both inverse and pseudo inverse of the matrix $\mathbf{A}$, as long as the dimensions are satisfied to proceed the operation. Also denote $[\mathbf{A}_1\ \mathbf{A}_2\ \cdots\ \mathbf{A}_N]$ as the horizontal concatenation of matrices from $\mathbf{A}_1$ to $\mathbf{A}_N$.

A. Approach on Transmitter Side with Cascaded Coder

This approach is similar to the design of [14]. Each BS uses a cascaded precoder to zero-forcing all inter-cell interferences (ICI) from other cells, and then deal with intra-cell interferences (IUI) in its own cell. The whole process takes four steps as following:

Step 1: Choose an auxiliary intermediate precoder $\mathbf{\Phi}_k \in \mathbb{C}^{N_t \times (M \cdot d)}$ at the k-th BS (transmitter), and a second precoder $\tilde{\mathbf{V}}_{k:m} \in \mathbb{C}^{(M \cdot d) \times d}$ preceding the first chosen precoder. Then the actual precoder $\mathbf{V}_{k:m}$ is composed of:

$$\mathbf{V}_{k:m} = \mathbf{\Phi}_k \tilde{\mathbf{V}}_{k:m} \quad m \in \mathcal{M}, k \in \mathcal{K} \tag{5}$$

(Notice the index k and m refer to all BSs and MSs, so that they could change accordingly.)

Step 2: When the first precoder $\mathbf{\Phi}_j$ is randomly picked, to enable zero-forcing the ICI from arbitrary k-th cell, all M users in the k-th cell should determine $\mathbf{U}_{k:m}$ to satisfy the following conditions (as mentioned, the index has changed for consistency of expressions):

$$\mathbf{U}_{k:m}^{\dagger} \underbrace{[\cdots\ \mathbf{H}_j^{k:m} \mathbf{\Phi}_j\ \cdots]}_{j \in \mathcal{K} \backslash \{k\}} = \mathbf{0} \quad m \in \mathcal{M} \tag{6}$$

To be feasible to find $\mathbf{U}_{k:m}$, the dimensions should satisfy $N_r \geq (K-1)Md + d$.

Step 3: Now observe each $\mathbf{\Phi}_k$ again, notice there're $(K-1)M$ zero-forcing conditions (notice the index as well):

$$\begin{bmatrix} \vdots \\ \mathbf{U}_{j:m}^{\dagger} \mathbf{H}_k^{j:m} \\ \vdots \end{bmatrix} \mathbf{\Phi}_k = \mathbf{0} \quad m \in \mathcal{M}, j \in \mathcal{K} \backslash \{k\} \tag{7}$$

Remark 1: Check the equation (7). Normally, it is feasible to find $\mathbf{\Phi}_k$ only when the dimensions satisfy $N_t \geq (K-1)Md + Md$. However, since (6) already guarantees this condition, it is only required that $N_t \geq Md$ in this specific design process. So this process naturally contains an *implicit* and *inherent* alignment.

Step 4: Then each k-th BS knows its equivalent downlink channel $\mathbf{U}_{k:m} \mathbf{H}_k^{k:m} \mathbf{\Phi}_k$ from each intra-cell MS. It forms zero-forcing transmit streams which could eliminate IUI between users, while it does not need to know the actual interfering streams. The second precoder matrix is obtained by an inverse operation (notice the index as well):

$$\left[\tilde{\mathbf{V}}_{k:1}\ \tilde{\mathbf{V}}_{k:2}\ \cdots\ \tilde{\mathbf{V}}_{k:M}\right] = \begin{bmatrix} \mathbf{U}_{k:1}^{\dagger} \mathbf{H}_k^{k:1} \mathbf{\Phi}_k \\ \mathbf{U}_{k:2}^{\dagger} \mathbf{H}_k^{k:2} \mathbf{\Phi}_k \\ \vdots \\ \mathbf{U}_{k:M}^{\dagger} \mathbf{H}_k^{k:M} \mathbf{\Phi}_k \end{bmatrix}^{-1} \tag{8}$$

In summary, the four steps determine all intermediate precoders, then receive filters, and finally second precoders, in sequence. Most important, alignment is implicitly contained in step 3 from the view of BS, which reflects the complicacy of IA in cellular networks.

B. Approach on Receiver Side with Cascaded Coder: I

This approach is proposed as a dual solution of the above approach on transmitter side. Set the cascaded coders on the receiver side. The whole process takes the following four steps:

Step 1: Choose an auxiliary or intermediate receive filter matrix $\mathbf{\Psi}_{k:m} \in \mathbb{C}^{N_r \times Md}$ at the m-th MS in the k-th cell, and a second receive filter $\tilde{\mathbf{U}}_{k:m} \in \mathbb{C}^{Md \times d}$ which precedes the first filter. Then the actual receive filter $\mathbf{U}_{k:m}$ is composed of:

$$\mathbf{U}_{k:m} = \mathbf{\Psi}_{k:m}\tilde{\mathbf{U}}_{k:m} \quad m \in \mathcal{M}, k \in \mathcal{K} \tag{9}$$

Step 2: When every first receive filter $\mathbf{\Psi}_{j:n}$ is randomly picked, to enable zero-forcing ICI, the k-th BS should determine $\mathbf{V}_{k:m}, m \in \mathcal{M}$ which satisfies the condition:

$$\begin{bmatrix} \vdots \\ \mathbf{\Psi}_{j:n}^{\dagger}\mathbf{H}_{k}^{j:n} \\ \vdots \end{bmatrix} [\mathbf{V}_{k:1}\ \mathbf{V}_{k:2}\ \cdots\ \mathbf{V}_{k:M}] = \mathbf{0} \quad n \in \mathcal{M}, j \in \mathcal{K}\backslash\{k\} \tag{10}$$

To be feasible to determine $[\mathbf{V}_{k:1}\ \mathbf{V}_{k:2}\ \cdots\ \mathbf{V}_{k:M}]$, the dimensions should satisfy $N_t \geq (K-1)M^2d + Md$.

Step 3: Now observe each $\mathbf{\Psi}_{k:m}$ again, notice there're $(K-1)M$ number of zero-forcing conditions:

$$\mathbf{\Psi}_{k:m}^{\dagger}[\underbrace{\cdots\ \mathbf{H}_{j}^{k:m}\mathbf{V}_{j:n}\ \cdots}_{n\in\mathcal{M}, j\in\mathcal{K}\backslash\{k\}}] = \mathbf{0} \quad m \in \mathcal{M} \tag{11}$$

Remark 2: Check the condition of (11). Notice in general it is only feasible to find $\mathbf{\Psi}_{k:m}$ when the dimensions satisfy $N_r \geq (K-1)Md + Md$. However, since (10) already guarantees the condition, it is only required that $N_r \geq Md$ in this specific design process. So this process naturally contains an *implicit* and *inherent* alignment.

Step 4: Then each intra-cell MS in the k-th cell knows its equivalent channel $\mathbf{\Psi}_{k:m}^{\dagger}\mathbf{H}_{k}^{k:m}\mathbf{V}_{k:m}$, while it does not know the actual interfering beams. It forms the zero-forcing receive filter to eliminate IUI. The second receive filter $\tilde{\mathbf{U}}_{k:m}$ is determined by an operation to find the null space:

$$\tilde{\mathbf{U}}_{k:m}^{\dagger}\left[\underbrace{\cdots\ \mathbf{\Psi}_{k:m}^{\dagger}\mathbf{H}_{k}^{k:m}\mathbf{V}_{k:n}\ \cdots}_{n\in\mathcal{M}\backslash\{m\}}\right] = \mathbf{0} \tag{12}$$

In summary, the four steps determine all intermediate receive filters, then precoders, and finally second receive filters, in sequence. Most important, alignment is implicitly contained in step 3 from the view of MS, which reflects the complicacy of IA in cellular networks.

C. Approach on Receiver Side with Cascaded Coder: II

This approach is similar to the design of [15]. Each MS uses a cascaded receive filter to align all inter-cell interferences (ICI) from other cells, and then deal with ICI and intra-cell interferences (IUI) in its own cell at the same time. The whole process takes four steps as following:

Step 1: For each m-th MS in k-th cell, the receive filter $\mathbf{U}_{k:m}$ is defined as two cascaded filter matrices:

$$\begin{aligned} &\mathbf{U}_{k:m} = \mathbf{G}_{k:m}^{\dagger}\Lambda_{\mathcal{K}:m} \\ &\mathbf{G}_{k:m} = [\underbrace{\mathbf{I}_{N_t}\cdots\mathbf{I}_{N_t}}_{K-1}][\underbrace{\cdots\ \mathbf{H}_{j}^{k:m}\ \cdots}_{j\in\mathcal{K}\backslash\{k\}}]^{-1} \\ &\text{So that}\ \ \mathbf{G}_{k:m} \in \mathbb{C}^{N_t \times N_r}, \mathbf{G}_{k:m}\mathbf{H}_{j}^{k:m} = \mathbf{I}_{N_t}\ \ \forall j \in \mathcal{K}\backslash\{k\} \end{aligned} \tag{13}$$

$\mathbf{G}_{k:m}$ is set that all ICI from any other j-th cell are aligned together. While $\Lambda_{\mathcal{K}:m}$ is a common filter set as the same for all cells in the set $\mathcal{K}$.

To be feasible to determine $\mathbf{G}_{k:m}$ by the inverse operation, the dimensions should satisfy $N_r \geq (K-1)N_t$.

Step 2: Since the common receive filter $\Lambda_{\mathcal{K}:m} \in \mathbb{C}^{N_t \times d}$ is set to be same for all cells of $\mathcal{K}$, the output stream as in the system equation (1) is presented as following:

$$\begin{aligned}\Lambda_{\mathcal{K}:m}^{\dagger}\mathbf{G}_{k:m}\mathbf{y}_{k:m} = \\ \Lambda_{\mathcal{K}:m}^{\dagger}\mathbf{G}_{k:m}\mathbf{H}_k^{k:m}\mathbf{V}_{k:m}\mathbf{x}_{k:m} + \sum_{n\neq m}^{n\in\mathcal{M}} \Lambda_{\mathcal{K}:m}^{\dagger}\mathbf{G}_{k:m}\mathbf{H}_k^{k:m}\mathbf{V}_{k:n}\mathbf{x}_{k:n} \\ + \sum_{j\neq k}^{j\in\mathcal{K}} \sum_{n\in\mathcal{M}} \Lambda_{\mathcal{K}:m}^{\dagger}\mathbf{V}_{j:n}\mathbf{x}_{j:n}\end{aligned} \tag{14}$$

To eliminate ICI and IUI terms in the equation (14) respectively, the zero-forcing conditions should be set as:

$$\begin{aligned}\Lambda_{\mathcal{K}:m}^{\dagger}\mathbf{G}_{k:m}\mathbf{H}_k^{k:m}\mathbf{V}_{k:n} = \mathbf{0} \quad n \in \mathcal{M}\backslash\{m\} \\ \Lambda_{\mathcal{K}:m}^{\dagger}\mathbf{V}_{j:n} = \mathbf{0} \quad j \in \mathcal{K}\backslash\{k\}, n \in \mathcal{M}\end{aligned} \tag{15}$$

Step 3: Then observe from k-th BS to choose the precoder $[\cdots \ \mathbf{V}_{k:m} \ \cdots]$, the zero-forcing conditions in equation (15) are equivalently presented with new indices in the following expression:

$$\begin{aligned}\Lambda_{\mathcal{K}:n}^{\dagger}\mathbf{G}_{k:n}\mathbf{H}_k^{k:n}\mathbf{V}_{k:m} = \mathbf{0} \quad n \in \mathcal{M}\backslash\{m\} \\ \Lambda_{\mathcal{K}:n}^{\dagger}\mathbf{V}_{k:m} = \mathbf{0} \quad n \in \mathcal{M}\end{aligned} \tag{16}$$

Step 4: So for each k-th BS, the precoder could be determined by only one inverse operation:

$$\mathbf{B}_k = \begin{bmatrix} \vdots & \\ \Lambda_{\mathcal{K}:m}^{\dagger}\mathbf{G}_{k:m}\mathbf{H}_k^{k:m} & \Big\} M \\ \vdots & \\ \vdots & \\ \Lambda_{\mathcal{K}:m}^{\dagger} & \Big\} M \\ \vdots & \end{bmatrix} \tag{17}$$

$$[\mathbf{V}_{k:1} \ \mathbf{V}_{k:2} \ \cdots \ \mathbf{V}_{k:M}] = \text{The first } Md \text{ columns of } \mathbf{B}_k^{-1}$$

Check that $[\mathbf{V}_{k:1} \ \mathbf{V}_{k:2} \ \cdots \ \mathbf{V}_{k:M}]$ indeed satisfies the conditions in (16).

Remark 3: To be feasible to obtain $[\mathbf{V}_{k:1} \ \mathbf{V}_{k:2} \ \cdots \ \mathbf{V}_{k:M}]$ by an inverse operation, the dimensions should satisfy $N_t \geq 2Md$. While in general cases, it is required that $N_t \geq KMd$. So this process naturally contains an *implicit* and *inherent* alignment.

In summary, the four steps determine all intermediate receive filters, and then precoders as well as second receive filters, in sequence. Most important, alignment is explicitly contained in step 1 from the view of BS.

D. Approach from Receiver Side with Direct Interplay

This approach is similar to the design of [18]. The alignment is jointly implemented on both BS(transmitter) side and MS(receiver) side via intricate and meticulous interplays and cooperations. The whole process takes two steps as following:

Step 1: Regarding channels from the k-th BS to all MSs in j-th cell, the equivalent receive filtered channel subspaces are set to be equal to a random predetermined reference subspace:

$$\begin{aligned}\mathbf{U}_{j:1}^{\dagger}\mathbf{H}_k^{j:1} = \mathbf{U}_{j:2}^{\dagger}\mathbf{H}_k^{j:2} = \cdots = \mathbf{U}_{j:M}^{\dagger}\mathbf{H}_k^{j:M} = (\mathbf{\Omega}_k^j)^{\dagger} \\ j \in \mathcal{K}\backslash\{k\}\end{aligned} \tag{18}$$

Remark 4: Notice the step of (18) is an *explicit* alignment of ICI from the k-th BS to all the MSs in the other j-th cell.

Observe from the MSs in the k-th cell, (change the indices accordingly) to satisfy the condition (18), $\mathbf{U}_{k:m}$ and $\mathbf{\Omega}_j^k$ could be found by solving a null space problem:

$$\left[\underbrace{\cdots\ (\mathbf{\Omega}_j^k)^\dagger\ \cdots}_{j\in\mathcal{K}\backslash\{k\}}\ \mathbf{U}_{k:1}^\dagger\ \mathbf{U}_{k:2}^\dagger\ \cdots\ \mathbf{U}_{k:M}^\dagger\right]\bullet \left[\begin{array}{cccc} \left.\begin{array}{cccc}\mathbf{I}_{N_t}\cdots\mathbf{I}_{N_t} & & & \\ & \mathbf{I}_{N_t}\cdots\mathbf{I}_{N_t} & & \\ & & \ddots & \\ & & & \mathbf{I}_{N_t}\cdots\mathbf{I}_{N_t}\end{array}\right\} K-1 \\ -\mathbf{H}_1^{k:1} & \cdots & -\mathbf{H}_j^{k:1} & \cdots\ -\mathbf{H}_K^{k:1} \\ -\mathbf{H}_1^{k:2} & \cdots & -\mathbf{H}_j^{k:2} & \cdots\ -\mathbf{H}_K^{k:2} \\ \ddots & \ddots & \ddots & \ddots\ \ddots \\ -\mathbf{H}_1^{k:M} & \cdots & -\mathbf{H}_j^{k:M} & \cdots\ -\mathbf{H}_K^{k:M}\end{array}\right] = \mathbf{0} \tag{19}$$

To be feasible to obtain $\mathbf{U}_{k:m}$ and $\mathbf{\Omega}_j^k$ via a null space operation, the dimensions should follow $(K-1)N_t + MN_r \geq (K-1)MN_t + d$.

Step 2: Thus for the k-th BS, the precoders are determined by the following inverse operation to eliminate both IUI and ICI:

$$[\ \cdots\ \mathbf{V}_{k:m}\ \cdots\ ] = \text{first } Md \text{ columns of } \left[\begin{array}{c}\left.\begin{array}{c}\vdots \\ \mathbf{U}_{k:m}^\dagger\mathbf{H}_k^{k:m} \\ \vdots\end{array}\right\} m\in\mathcal{M} \\ \left.\begin{array}{c}\vdots \\ \mathbf{\Omega}_k^{j\,\dagger} \\ \vdots\end{array}\right\} j\in\mathcal{K}\backslash\{k\}\end{array}\right]^{-1} \tag{20}$$

To be feasible to obtain $[\ \cdots\ \mathbf{V}_{k:m}\ \cdots\ ]$ via the inverse operation, the dimensions should satisfy $N_t \geq Md + (K-1)d$.

Check the equation (20) and find that $[\ \cdots\ \mathbf{V}_{k:m}\ \cdots\ ]$ indeed eliminate the IUI between each other in the cell and ICI to other cells.

In summary, the two steps determine all receive filters and aligned subspace and then precoders in sequence. Most important, alignment is explicitly implemented in step 1 on the MS side, and implicitly implemented by an inverse operation in step 2 on the BS side. Compared with previous approaches, notice their alignment are only on one side. So that this approach has the advantage of saving antenna usage and obtaining higher DoF. The disadvantage is the corresponding increased CSI exchange.

E. Approach from Transmitter Side with Direct Interplay

This approach is proposed as a dual solution of the above approach on receiver side. Here make the explicit alignment from the BS side. The whole process takes the following two steps:

Step 1: Regarding channels from arbitrary j-th BS to all MSs in the k-th cell, all the equivalent precoded channel subspaces are set to be equal to a random predetermined reference subspace:

$$\underbrace{\cdots = \mathbf{H}_j^{k:m}[\mathbf{V}_{j:1}\cdots\mathbf{V}_{j:M}] = \cdots}_{j\in\mathcal{K}\backslash\{k\}} = \mathbf{\Theta}^{k:m} \tag{21}$$

Remark 5: Notice the step of (21) is an *explicit* alignment of ICI from all the BSs in other cells to each m-th MS in the k-th cell.

Observe from all the BSs, (change the indices accordingly) to satisfy the condition (21), $[\mathbf{V}_{k:1}\cdots\mathbf{V}_{k:M}]$ and $\mathbf{\Theta}^{k:m}$ could be found by solving the following null space problem:

$$\left[\begin{array}{cc}
\left.\begin{array}{cc}\mathbf{I}_{N_r} & \ddots \\ \vdots & -\mathbf{H}_j^{1:m} \\ \mathbf{I}_{N_r} & \ddots \end{array}\right\} j\in\mathcal{K}\backslash\{1\} & \\
\ddots \quad\quad \vdots & \\
\left.\begin{array}{cc}\mathbf{I}_{N_r} & \ddots \\ \vdots & -\mathbf{H}_j^{k:m} \\ \mathbf{I}_{N_r} & \ddots \end{array}\right\} j\in\mathcal{K}\backslash\{k\} & \\
\ddots \quad\quad \vdots & \\
\left.\begin{array}{cc}\mathbf{I}_{N_r} & \ddots \\ \vdots & -\mathbf{H}_j^{K:m} \\ \mathbf{I}_{N_r} & \ddots \end{array}\right\} j\in\mathcal{K}\backslash\{K\} & \\
\ddots \quad\quad \vdots &
\end{array}\right\} m\in\mathcal{M}$$

$$\bullet\left[\begin{array}{c}
\vdots \\ \left.\begin{array}{c}\mathbf{\Theta}^{k:m}\\ \vdots\end{array}\right\} k\in\mathcal{K} \\ \vdots \\ \vdots \\ \left.\begin{array}{c}[\mathbf{V}_{k:1}\cdots\mathbf{V}_{k:M}]\\ \vdots\end{array}\right\} k\in\mathcal{K}
\end{array}\right\} m\in\mathcal{M} = \mathbf{0} \tag{22}$$

To be feasible to obtain $[\mathbf{V}_{k:1}\cdots\mathbf{V}_{k:M}]$ and $\mathbf{\Theta}^{k:m}$ via a null space operation, the dimensions should follow $KMN_r+KN_t \geq K(K-1)MN_r + Md$.

Step 2: Thus for the m-th MS in k-th cell, its receive filter is determined via a null space operation to eliminate both IUI and ICI:

$$\mathbf{U}_{k:m}^{\dagger}\left[\begin{array}{cc}\mathbf{H}_k^{k:m}\big[\underbrace{\cdots\ \mathbf{V}_{k:n}\ \cdots}_{n\in\mathcal{M}\backslash\{m\}}\big] & \mathbf{\Theta}^{k:m}\end{array}\right] = \mathbf{0} \tag{23}$$

To be feasible to obtain $\mathbf{U}_{k:m}$, the dimensions should follow $N_r \geq (M-1)d + Md + d$. It is also easy to check that the condition (23) directly eliminates both IUI and ICI.

In summary, the two steps determine all precoders and aligned subspace and then receive filters in sequence. Most important, alignment is explicitly implemented in step 1 on the BS side by a null space operation. Notice that when the MS chooses a receive filter $\mathbf{U}_{k:m}$ it needs not to concern about independency with receive filters in other MSs thanks to its distributed nature, while when the BS chooses the precoders $\mathbf{V}_{k:n}$ designated to multiple MSs it needs to concern their independency to form the subspace.

F. Comparison of System Conditions

For all the proposed new approaches of multi-cell downlink interference alignment, the system require different level of conditions to support the implementations. There are three main aspects to look into and compare. The first aspect is the usage of antennas for both BS and MS nodes. The number of antennas limit the achievable DoF for each node. The second aspect is

Approach	Minimum BS Antenna.	Minimum MS Antenna
A	Md	$(K-1)Md+d$
B	$(K-1)M^2d+Md$	Md
C	$2Md$	$(K-1)2Md$
D	$(M+K-1)d$	$(K-1)\frac{(M-1)}{M}(M+K-1)d$ $+d/M$
E	$(KM-2M)2Md$ $+(M/K)d$	$2Md$

TABLE I
MINIMUM ANTENNA USAGE FOR BSS AND MSS IN ALL APPROACHES IN MODEL 1

the CSI for the nodes to obtain channel knowledge. The CSI causes system overhead which would degrade the performance to some extent, and proper tradeoff could be made to treat the system as a whole. The third aspect is the computational complexity for the nodes to calculate necessary coders. The complexity impact on the system factors such as delay, power, hardware etc., and it is expected to be the lower the better.

1) DoF and Antenna Range: In general, the feasibility conditions of cellular networks are still not solved so far, i.e. the minimum number of antennas required to obtain intended DoF is not known. For example, [11] provides a special case in which each MS receives a single beam so that the antennas should satisfy $N_r+N_t \geq M(K+1)$ in a K-cell network with M users in each cell where N_r and N_t are the numbers of MS(receive) antennas and BS(transmit) antennas respectively. While in the example of [18], each BS and MS have N_t and N_r antennas respectively, and satisfy the condition $3N_r/2 < N_t < 2N_r$ to achieve a final $2N_r$ DoF in the two-cell network. It shows that the number of antennas plays a key role to implement alignment. Moreover, in an extreme case, if all nodes are provided with unlimited number of antennas, each node could trivially proceed interference cancellation via perfect zero-forcing with sufficient antennas.

The aim of this work is to exploit interference alignment in the network with limited provision of antennas at both BS and MS nodes, and also to look into the balance between the BS side and MS side to implement alignment to obtain DoF with a reasonable number antennas in the system. For the above five approaches, all the antenna configurations are listed in Table I, in which the notations of 'A', 'B', 'C', 'D', and 'E' denote the proposed five approaches in sequence.

In summary, as shown in Table I, approach 'B' and approach 'E' need a large number of antennas at BS nodes, while approach 'A', 'C' and 'D' need a large number of antennas at MS nodes.

2) CSI and Overhead: Although the design of interference alignment provides a promising DoF in theory, it still has to face the challenge of realistic implementation. It is required that all BSs and all MSs should know a certain level of channel state information (CSI), so that the alignment could be made with operations of the channel matrices. Usually, CSI could be acquired by five key steps: common forward link training [23], [2]; channel quantization [32]; channel feedback [33]; beamformer selection; dedicated training. Furthermore, there is a tradeoff between the overhead to obtain CSI and the effective DoF.

The aim of this work is to provide a comparison of CSI requirements for all nodes in different approaches. For the above five approaches, all the CSI configurations are listed in Table II, in which the notations of 'A', 'B', 'C', 'D', and 'E' denote the proposed five approaches in sequence. The CSI configurations for BSs and MSs are displayed separately, and the corresponding descriptions include its source, its content, and the quantity.

In summary, as shown in Table II, approach 'B' and approach 'E' need a large amount of CSI. In addition, approach 'B', 'D' and 'E' need inter-cell CSI for BSs, and approach 'A', 'C', 'D' need inter-cell CSI for MSs. In general, inter-cell CSI are much harder to obtain than intra-cell CSI. So it is suggested that BSs and MSs only utilize feedback within a cell, i.e. local CSI as in [14], with a few changes to the existing intra-cell feedback mechanism for multi-user MIMO. When BSs need global CSI or inter-cell CSI, direct feedback from inter-cell communication sessions or backhaul cooperations are necessary. Due to the nature of broadcast channels, BSs and MSs have different demands for CSI. The MSs could share CSI in the cell. BSs and MSs could exchange CSI via back-and-forth signalling. Collaborative BSs could be coordinated with the multi-cell processing (MCP) strategy as in [29]. MSs are also allowed to cooperate via conferencing [29].

3) Computational Complexity: To implement the design of interference alignment, all nodes need to calculate their coding matrices or filters with obtained channel state information (CSI). To obtain different kinds of results with different types of operations, all the nodes need to evaluate their system cost by a universal metric, i.e. computational complexity. The computational complexity is counted as the number of flops. While a flop usually refers to a floating point operation as addition, multiplication, or division of real numbers, so that a complex addition and multiplication have two flops and six flops, respectively [34] [35].

The aim of this work is to provide a comparison of requirements of computational complexities for all the nodes in different approaches. For the above five approaches, all the complexity configurations are listed in Table III. The notations 'A', 'B',

Approach	required CSI at k-th BS		
	Source	Content	Quantity
A	all intra-cell MSs	$\mathbf{U}_{k:m}^{\dagger}\mathbf{H}_{k}^{k:m}$	M
B	all inter-cell MSs	$\mathbf{\Psi}_{j:n}^{\dagger}\mathbf{H}_{k}^{j:n}$	$(K-1)M$
C	all intra-cell MSs	$\mathbf{G}_{k:m}\mathbf{H}_{k}^{k:m}$	M
D	all intra-cell MSs other inter-cell MSs	$\mathbf{U}_{k:m}^{\dagger}\mathbf{H}_{k}^{k:m}$,$\mathbf{\Omega}_{k}^{j}$	M,$K-1$
E	all inter-cell MSs	$\mathbf{H}_{k}^{j:m}$	$(K-1)M$ (excl. backhaul)

Approach	required CSI at m-th MS in k-th cell		
	Source	Content	Quantity
A	all inter-cell BSs	$\mathbf{H}_{j}^{k:m}\mathbf{\Phi}_{j}$	$(K-1)$
B	intra-cell BS	$\mathbf{H}_{k}^{k:m}\mathbf{V}_{k:n}$	$(M-1)$
C	all inter-cell BSs	$\mathbf{H}_{j}^{k:m}$	$(K-1)$
D	all inter-cell BSs	$\mathbf{H}_{j}^{k:m}$	$(K-1)$ (excl. conferencing)
E	intra-cell BS	$\mathbf{H}_{k}^{k:m}\mathbf{V}_{k:n}$,$\mathbf{\Theta}^{k:m}$	$(M-1),1$

TABLE II
CSI FOR BSS AND MSS IN ALL APPROACHES IN MODEL 1

'C', 'D', 'E' denote the proposed five approaches in sequence. The requirements for BS and MS are separately displayed. To calculate the target, two operations are available: matrix inverse and null space. The amount of calculation is also affected by the scales or sizes of the matrices.

Approach	expended Complexity at k-th BS		
	Target	Operation	Scale
A	$\tilde{\mathbf{V}}_{k:m}$	matrix inverse	$Md \times Md$
B	$\mathbf{V}_{k:m}$	null space	$N_t \times Md$
C	$\mathbf{V}_{k:m}$	matrix inverse	$2Md \times N_t$
D	$\mathbf{V}_{k:m}$	matrix inverse	$(M+K-1)d \times N_t$
E	$\mathbf{V}_{k:m}$, $\mathbf{\Theta}^{k:m}$	null space	$(KMN_r + KN_t) \times Md$

Approach	expended Complexity at m-th MS in k-th cell		
	Target	Operation	Scale
A	$\mathbf{U}_{k:m}$	null space	$N_r \times d$
B	$\tilde{\mathbf{U}}_{k:m}$	null space	$Md \times d$
C	$\mathbf{G}_{k:m}$	matrix inverse	$N_r \times (K-1)N_t$
D	$\mathbf{U}_{k:m}$,$\mathbf{\Omega}_{j}^{k}$	null space	$[(K-1)N_t + MN_r] \times d$
E	$\mathbf{U}_{k:m}$	null space	$N_r \times d$

TABLE III
COMPLEXITY FOR BSS AND MSS IN ALL APPROACHES IN MODEL 1

In summary, as shown in Table III, approach 'D' and 'E' need a large amount of complexity at BSs for operations with large scales, and approach 'C' and 'D' need a large amount of complexity at MSs for operations with large scales.

IV. BASIC DESIGN AND ANALYSIS OF MODEL 2

This section looks into model 2 as shown in Fig. 2 and equation (2). Each BS only affects MSs in two adjacent cells and vice versa each MS only receives inter-cell interference from two BSs in adjacent cells. In practical cellular networks, if the BS in one cell is not nearby MSs in another cell, then the interference could be negligible considering large path loss. So that the network is not fully connected, and could be modeled as an infinite cyclic network, in particular a Wyner model [24]. The Wyner model provides a simple and analytical tractable framework for a cellular system to capture the essence of inter-cell interference and fading. Previous extensive studies on the Wyner model mostly treat interference as noise [29], [36]. However in this work, the focus is on the DoF structure of interference in this cellular network. Similar to the analysis for model 1, in general, there are three angles to implement the design, i.e. on the BS side, on the MS side, and interplay on both BS and MS sides. Accordingly the following work proposes five approaches to implement the alignment.

Clarification: Be advised that, the notation settings are similar to the analysis for model 1, and some symbols are reused so long as they do not cause any confusion. In the following expressions of the design process, when a same BS or MS in a set is referred, the index may change between successive steps according to its subject or object position in the context of the current step. In each step, the index refers to all equal nodes. Specifically, k is used to denote the subject, and j is used to denote the object. Besides, in the corresponding tables, the index may also change according to the context of discussion.

A. Approach on Transmitter Side with Cascaded Coder

This approach is similar to the design of [14] as used in model 1. Each BS uses a cascaded precoder to zero-forcing ICI, and then deal with its own IUI. The whole process takes four steps as following:

Step 1: Choose an auxiliary intermediate precoder $\mathbf{\Phi}_k \in \mathbb{C}^{N_t \times (M \cdot d)}$ at k-th BS (transmitter), and a second precoder $\tilde{\mathbf{V}}_{k:m} \in \mathbb{C}^{(M \cdot d) \times d}$ preceding the first chosen precoder. Then the actual precoder $\mathbf{V}_{k:m}$ is composed of:

$$\mathbf{V}_{k:m} = \mathbf{\Phi}_k \tilde{\mathbf{V}}_{k:m} \quad m \in \mathcal{M}, k \in \mathcal{K} \tag{24}$$

(Notice the index refers to all equal nodes.)

Step 2: When the first precoder $\mathbf{\Phi}_j$ is randomly picked, to enable zero-forcing the ICI from the two adjacent cells, all M users in k-th cell should determine $\mathbf{U}_{k:m}$ to satisfy the following conditions (index changed):

$$\mathbf{U}_{k:m}^{\dagger}[\ \mathbf{H}_{k-1}^{k:m}\mathbf{\Phi}_{k-1}\ \mathbf{H}_{k+1}^{k:m}\mathbf{\Phi}_{k+1}\ ] = \mathbf{0} \quad m \in \mathcal{M} \tag{25}$$

To be feasible to find $\mathbf{U}_{k:m}$, the dimensions should satisfy $N_r \geq 2Md + d$. Obviously, this requirement is greatly loosened compared with the analysis for model 1, the full connected network.

Step 3: Now observe each $\mathbf{\Phi}_k$ again, notice there're $2M$ zero-forcing conditions to satisfy (notice index):

$$\begin{bmatrix} \vdots \\ \mathbf{U}_{k-1:m}^{\dagger}\mathbf{H}_k^{k-1:m} \\ \vdots \\ \vdots \\ \mathbf{U}_{k+1:m}^{\dagger}\mathbf{H}_k^{k+1:m} \\ \vdots \end{bmatrix} \mathbf{\Phi}_k = \mathbf{0} \quad m \in \mathcal{M} \tag{26}$$

Remark 6: Check the equation (26). Normally it is feasible to find $\mathbf{\Phi}_k$ only when $N_t \geq 2Md + Md$. However, since (25) already guarantees this condition, it is only required that $N_t \geq Md$ in this specific design process. So this process naturally contains an *implicit* and *inherent* alignment.

Step 4: Then each k-th BS knows its equivalent downlink channel $\mathbf{U}_{k:m}\mathbf{H}_k^{k:m}\mathbf{\Phi}_k$ from each intra-cell MS. It forms zero-forcing transmit streams eliminating IUI, without knowing the actual interfering streams. The second precoder matrix is obtained by an inverse operation (notice index):

$$\begin{bmatrix} \tilde{\mathbf{V}}_{k:1}\ \tilde{\mathbf{V}}_{k:2}\ \cdots\ \tilde{\mathbf{V}}_{k:M} \end{bmatrix} = \begin{bmatrix} \mathbf{U}_{k:1}^{\dagger}\mathbf{H}_k^{k:1}\mathbf{\Phi}_k \\ \mathbf{U}_{k:2}^{\dagger}\mathbf{H}_k^{k:2}\mathbf{\Phi}_k \\ \vdots \\ \mathbf{U}_{k:M}^{\dagger}\mathbf{H}_k^{k:M}\mathbf{\Phi}_k \end{bmatrix}^{-1} \tag{27}$$

In summary, the four steps determine intermediate precoders, receive filters, and second precoders in sequence. Alignment is implicitly contained in step 3. Compared with model 1, it is evident that less antennas are used here to implement alignment because of the connectivity only between neighboring cells.

B. Approach on Receiver Side with Cascaded Coder: I

This approach is proposed as a dual solution of the above approach on transmitter side. Set the cascaded coders on the receiver side. Then the whole process takes the following four steps:

Step 1: Choose an auxiliary or intermediate receive filter matrix $\mathbf{\Psi}_{k:m} \in \mathbb{C}^{N_r \times Md}$ at the m-th MS in the k-th cell, and a second receive filter $\tilde{\mathbf{U}}_{k:m} \in \mathbb{C}^{Md \times d}$ which precedes the first filter. Then the actual receive filter $\mathbf{U}_{k:m}$ is composed of:

$$\mathbf{U}_{k:m} = \mathbf{\Psi}_{k:m}\tilde{\mathbf{U}}_{k:m} \quad m \in \mathcal{M}, k \in \mathcal{K} \tag{28}$$

Step 2: When every first receive filter $\mathbf{\Psi}_{j:n}$ is randomly picked, to enable zero-forcing ICI, the k-th BS should determine $\mathbf{V}_{k:m}, m \in \mathcal{M}$ which satisfies the condition:

$$\begin{bmatrix} \vdots \\ \mathbf{\Psi}_{k-1:n}^{\dagger}\mathbf{H}_{k}^{k-1:n} \\ \vdots \\ \vdots \\ \mathbf{\Psi}_{k+1:n}^{\dagger}\mathbf{H}_{k}^{k+1:n} \\ \vdots \end{bmatrix} [\mathbf{V}_{k:1}\ \mathbf{V}_{k:2}\ \cdots\ \mathbf{V}_{k:M}] = \mathbf{0} \quad n \in \mathcal{M} \tag{29}$$

To be feasible to determine $[\mathbf{V}_{k:1}\ \mathbf{V}_{k:2}\ \cdots\ \mathbf{V}_{k:M}]$, the dimensions should satisfy $N_t \geq 2M^2d + Md$. Compared with model 1, the requirement for antennas is greatly reduced.

Step 3: Now observe each $\mathbf{\Psi}_{k:m}$ again, notice there're $2M$ zero-forcing conditions:

$$\mathbf{\Psi}_{k:m}^{\dagger}[\underbrace{\cdots\ \mathbf{H}_{k-1}^{k:m}\mathbf{V}_{k-1:n}\ \cdots\ \cdots\ \mathbf{H}_{k+1}^{k:m}\mathbf{V}_{k+1:n}\ \cdots}_{n\in\mathcal{M}}] = \mathbf{0} \qquad m \in \mathcal{M} \tag{30}$$

Remark 7: Check the condition of (30). Notice in general it is only feasible to find $\mathbf{\Psi}_{k:m}$ when the dimensions satisfy $N_r \geq 2Md + Md$. However, since (29) already guarantees the condition, it is only required that $N_r \geq Md$ in this specific design process. So this process naturally contains an *implicit* and *inherent* alignment.

Step 4: Then each intra-cell MS in the k-th cell knows its equivalent channel $\mathbf{\Psi}_{k:m}^{\dagger}\mathbf{H}_{k}^{k:m}\mathbf{V}_{k:m}$, while it does not know the actual interfering beams. It forms the zero-forcing receive filter to eliminate IUI. The second receive filter $\tilde{\mathbf{U}}_{k:m}$ is determined by an operation to find the null space:

$$\tilde{\mathbf{U}}_{k:m}^{\dagger}\left[\underbrace{\cdots\ \mathbf{\Psi}_{k:m}^{\dagger}\mathbf{H}_{k}^{k:m}\mathbf{V}_{k:n}\ \cdots}_{n\in\mathcal{M}\setminus\{m\}}\right] = \mathbf{0} \tag{31}$$

In summary, the four steps determine intermediate receive filters, precoders, second receive filters in sequence. Alignment is implicitly contained in step 3. Compared with model 1, the usage of antennas is evidently reduced because of the loose connectivity.

C. Approach on Receiver Side with Cascaded Coder: II

This approach is similar to the design of [15]. Each MS uses a cascaded receive filter to align ICI from other cells, and deal with ICI and IUI in its own cell. The whole process takes four steps as following:

Step 1: For each m-th MS in k-th cell, the receive filter $\mathbf{U}_{k:m}$ is defined as two cascaded filter matrices:

$$\begin{aligned} &\mathbf{U}_{k:m} = \mathbf{G}_{k:m}^{\dagger}\Lambda_{\mathcal{K}:m} \\ &\mathbf{G}_{k:m} = [\mathbf{I}_{N_t}\mathbf{I}_{N_t}][\mathbf{H}_{k-1}^{k:m}\ \mathbf{H}_{k+1}^{k:m}]^{-1} \\ &\text{So that}\ \ \mathbf{G}_{k:m} \in \mathbb{C}^{N_t \times N_r}, \mathbf{G}_{k:m}\mathbf{H}_{j}^{k:m} = \mathbf{I}_{N_t} \\ &\qquad\qquad\qquad\qquad \forall j = k-1, k+1 \end{aligned} \tag{32}$$

$\mathbf{G}_{k:m}$ is set to make all ICI from the two neighboring cells aligned together. While $\Lambda_{k:m}$ is a common filter set to be the same for all cells in the network.

To be feasible to determine $\mathbf{G}_{k:m}$ by the inverse operation, the dimensions should satisfy $N_r \geq 2N_t$. Compared with model 1, it is obvious that this condition is greatly loosened to save a lot of antennas.

Step 2: Since the common receive filter $\Lambda_{\mathcal{K}:m} \in \mathbb{C}^{N_t \times d}$ is set to be the same for all cells of $\mathcal{K}$, the output stream of (2) is presented as following:

$$\begin{aligned}\Lambda_{\mathcal{K}:m}^{\dagger}\mathbf{G}_{k:m}\mathbf{y}_{k:m} = \\ \Lambda_{\mathcal{K}:m}^{\dagger}\mathbf{G}_{k:m}\mathbf{H}_k^{k:m}\mathbf{V}_{k:m}\mathbf{x}_{k:m} + \sum_{n\neq m}^{n\in\mathcal{M}} \Lambda_{\mathcal{K}:m}^{\dagger}\mathbf{G}_{k:m}\mathbf{H}_k^{k:m}\mathbf{V}_{k:n}\mathbf{x}_{k:n} \\ + \sum_{j=k-1,k+1}\sum_{n\in\mathcal{M}} \Lambda_{\mathcal{K}:m}^{\dagger}\mathbf{V}_{j:n}\mathbf{x}_{j:n}\end{aligned} \tag{33}$$

To eliminate ICI and IUI terms in equation (33) respectively, the zero-forcing conditions should be set as:

$$\begin{aligned}\Lambda_{\mathcal{K}:m}^{\dagger}\mathbf{G}_{k:m}\mathbf{H}_k^{k:m}\mathbf{V}_{k:n} = \mathbf{0} \quad n \in \mathcal{M}\backslash\{m\} \\ \Lambda_{\mathcal{K}:m}^{\dagger}\mathbf{V}_{j:n} = \mathbf{0} \quad j = k-1, k+1, n \in \mathcal{M}\end{aligned} \tag{34}$$

Compared with model 1, the condition is loosened.

Step 3: Then observe from k-th BS to choose the precoder $[\cdots \ \mathbf{V}_{k:m} \ \cdots]$, the zero-forcing conditions in equation (34) are equivalently presented with new indices in the following expression:

$$\begin{aligned}\Lambda_{\mathcal{K}:n}^{\dagger}\mathbf{G}_{k:n}\mathbf{H}_k^{k:n}\mathbf{V}_{k:m} = \mathbf{0} \quad n \in \mathcal{M}\backslash\{m\} \\ \Lambda_{\mathcal{K}:n}^{\dagger}\mathbf{V}_{k:m} = \mathbf{0} \quad n \in \mathcal{M}\end{aligned} \tag{35}$$

Step 4: So for each k-th BS, the precoder could be determined by only one inverse operation:

$$\mathbf{B}_k = \begin{bmatrix} \vdots & \\ \Lambda_{\mathcal{K}:m}^{\dagger}\mathbf{G}_{k:m}\mathbf{H}_k^{k:m} & \Big\} M \\ \vdots & \\ \vdots & \\ \Lambda_{\mathcal{K}:m}^{\dagger} & \Big\} M \\ \vdots & \end{bmatrix} \tag{36}$$

$$[\mathbf{V}_{k:1} \ \mathbf{V}_{k:2} \ \cdots \ \mathbf{V}_{k:M}] = \text{The first } Md \text{ columns of } \mathbf{B}_k^{-1}$$

Check that $[\mathbf{V}_{k:1} \ \mathbf{V}_{k:2} \ \cdots \ \mathbf{V}_{k:M}]$ indeed satisfies the conditions in (35).

Remark 8: To be feasible to obtain $[\mathbf{V}_{k:1} \ \mathbf{V}_{k:2} \ \cdots \ \mathbf{V}_{k:M}]$ by an inverse operation, the dimensions should satisfy $N_t \geq 2Md$. While in general cases, it is required that $N_t \geq Md + 2Md$ for the BS to handle interferences to two adjacent cells. So this process naturally contains an *implicit* and *inherent* alignment.

In summary, the four steps determine all receive filters, precoders and second receive filters in sequence. Alignment is explicitly implemented in step 1. Compared with model 1, less antennas are required to implement alignment because of the loose connectivity.

D. Approach from Receiver Side with Direct Interplay

This approach is similar to the design of [18]. The alignment is jointly implemented on both BS(transmitter) side and MS(receiver) side via intricate and meticulous interplays and cooperations. The whole process takes two steps as following:

Step 1: Regarding channels from the k-th BS to all MSs in j-th cell, the equivalent receive filtered channel subspaces are set to be equal to a random pre-determined reference subspace:

$$\begin{aligned}\mathbf{U}_{j:1}^{\dagger}\mathbf{H}_k^{j:1} = \mathbf{U}_{j:2}^{\dagger}\mathbf{H}_k^{j:2} = \cdots = \mathbf{U}_{j:M}^{\dagger}\mathbf{H}_k^{j:M} = (\mathbf{\Omega}_k^j)^{\dagger} \\ j = k-1, k+1\end{aligned} \tag{37}$$

Remark 9: Notice the step of (37) is an *explicit* alignment of ICI from the the k-th BS to all MSs only in the two adjacent cells.

Observe from all MSs in k-th cell, (index changed) to satisfy the condition (37), $\mathbf{U}_{k:m}$, $\mathbf{\Omega}_{k-1}^{k}$ and $\mathbf{\Omega}_{k+1}^{k}$ could be found by solving the following null space problem:

$$\begin{bmatrix}(\mathbf{\Omega}_{k-1}^{k})^{\dagger} & (\mathbf{\Omega}_{k+1}^{k})^{\dagger} & \mathbf{U}_{k:1}^{\dagger} & \mathbf{U}_{k:2}^{\dagger} & \cdots & \mathbf{U}_{k:M}^{\dagger}\end{bmatrix} \bullet \begin{bmatrix} \mathbf{I}_{N_t} \cdots \mathbf{I}_{N_t} & \\ & \mathbf{I}_{N_t} \cdots \mathbf{I}_{N_t} \\ -\mathbf{H}_{k-1}^{k:1} & -\mathbf{H}_{k+1}^{k:1} \\ -\mathbf{H}_{k-1}^{k:2} & -\mathbf{H}_{k+1}^{k:2} \\ \ddots & \ddots \\ -\mathbf{H}_{k-1}^{k:M} & -\mathbf{H}_{k+1}^{k:M} \end{bmatrix} = \mathbf{0} \tag{38}$$

To be feasible to obtain $\mathbf{U}_{k:m}$, $\mathbf{\Omega}_{k-1}^{k}$ and $\mathbf{\Omega}_{k+1}^{k}$ via a null space operation, the dimensions should follow $2N_t + MN_r \geq 2MN_t + d$. Compared with model 1, the condition is greatly loosened, and a lot of antennas could be saved.

Step 2: Thus for the k-th BS, the precoders are determined by the following inverse operation to eliminate both IUI and ICI:

$$[\ \cdots\ \mathbf{V}_{k:m}\ \cdots\ ] = \text{first } Md \text{ columns of} \begin{bmatrix} \vdots \\ \mathbf{U}_{k:m}^{\dagger}\mathbf{H}_{k}^{k:m} \\ \vdots \end{bmatrix} m \in \mathcal{M} \\ (\mathbf{\Omega}_{k}^{k-1})^{\dagger} \\ (\mathbf{\Omega}_{k}^{k+1})^{\dagger} \end{bmatrix}^{-1} \tag{39}$$

To be feasible to obtain $[\ \cdots\ \mathbf{V}_{k:m}\ \cdots\ ]$ via the inverse operation, the dimensions should satisfy $N_t \geq Md + 2d$. Compared with model 1, the condition is loosened to save a number of antennas.

Check the equation (39) and find that $[\ \cdots\ \mathbf{V}_{k:m}\ \cdots\ ]$ indeed eliminate the IUI in the cell and ICI to the two adjacent cells.

In summary, the two steps determine receive filters, aligned subspace and precoders in sequence. Alignment is implemented on the MS side and BS side. Compared with model 1, the requirement for antennas are greatly reduced because of the loose connectivity.

E. Approach from Transmitter Side with Direct Interplay

This approach is proposed as a dual solution of the above approach on receiver side. It implements the alignment on the BS side. The whole process takes the following two steps:

Step 1: Regarding channels from the two adjacent $(k-1)$-th and $(k+1)$-th BS to all MS in k-th cell, the two equivalent precoded channel subspaces are set to be equal to a random predetermined reference subspace:

$$\mathbf{H}_{k-1}^{k:m}[\mathbf{V}_{k-1:1} \cdots \mathbf{V}_{k-1:M}] = \mathbf{H}_{k+1}^{k:m}[\mathbf{V}_{k+1:1} \cdots \mathbf{V}_{k+1:M}] = \mathbf{\Theta}^{k:m} \tag{40}$$

Remark 10: Notice the step of (40) is an *explicit* alignment of ICI from the two adjacent BSs to m-th MS in the k-th cell. Observe from the side of all BSs, (index changed) to satisfy the condition (40), $[\mathbf{V}_{k:1} \cdots \mathbf{V}_{k:M}]$ and $\mathbf{\Theta}^{k:m}$ could be found

by solving the following null space problem:

$$\begin{bmatrix} \left.\begin{matrix} \mathbf{I}_{N_r} & & -\mathbf{H}_K^{1:m} \\ \mathbf{I}_{N_r} & & -\mathbf{H}_2^{1:m} \end{matrix}\right\} m\in\mathcal{M} \\ \begin{matrix} \ddots & & \vdots \end{matrix} \\ \left.\begin{matrix} \mathbf{I}_{N_r} & & -\mathbf{H}_{k-1}^{k:m} \\ \mathbf{I}_{N_r} & & -\mathbf{H}_{k+1}^{k:m} \end{matrix}\right\} m\in\mathcal{M} \\ \begin{matrix} \ddots & & \vdots \end{matrix} \\ \left.\begin{matrix} \mathbf{I}_{N_r} & & -\mathbf{H}_{K-1}^{K:m} \\ \mathbf{I}_{N_r} & & -\mathbf{H}_{K+1}^{K:m} \end{matrix}\right\} m\in\mathcal{M} \\ \begin{matrix} \ddots & & \vdots \end{matrix} \end{bmatrix} \tag{41}$$

$$\bullet \begin{bmatrix} \left.\begin{matrix} \vdots \\ \boldsymbol{\Theta}^{k:m} \\ \vdots \end{matrix}\right\} k\in\mathcal{K} \\ \vdots \\ \left.\begin{matrix} \vdots \\ [\mathbf{V}_{k:1}\cdots\mathbf{V}_{k:M}] \\ \vdots \end{matrix}\right\} k\in\mathcal{K} \end{bmatrix} m\in\mathcal{M} = \mathbf{0}$$

To be feasible to obtain $[\mathbf{V}_{k:1}\cdots\mathbf{V}_{k:M}]$ and $\boldsymbol{\Theta}^{k:m}$ via a null space operation, the dimensions should follow $KMN_r+KN_t \geq 2KMN_r + Md$. Compared with model 1, the condition is greatly loosened.

Step 2: Thus for the m-th MS in k-th cell, its receive filter is determined via a null space operation to eliminate both IUI and ICI:

$$\mathbf{U}_{k:m}^{\dagger}\begin{bmatrix} \mathbf{H}_k^{k:m}\big[\underbrace{\cdots\ \mathbf{V}_{k:n}\ \cdots}_{n\in\mathcal{M}\setminus\{m\}}\big] & \boldsymbol{\Theta}^{k:m} \end{bmatrix} = \mathbf{0} \tag{42}$$

To be feasible to obtain $\mathbf{U}_{k:m}$, the dimensions should follow $N_r \geq (M-1)d+Md+d$. It is easy to check that the condition (42) directly eliminates both IUI and ICI.

In summary, the two steps determine precoders, aligned subspaces, and receive filters in sequence. Alignment is explicitly implemented. Compared with model 1, the antennas for BS nodes are greatly reduced because of the loose connectivity.

F. Comparison of System Conditions

Similar to the analyses for model 1, system conditions are listed and compared for all the proposed five approaches of downlink interference alignment in a Wyner-type cellular network with two adjacent links for each cell. There are three aspects to investigate: the usage of antennas which is related to available DoF; the CSI required which may generate overhead in the system; the computational complexity which impacts realistic performances.

1) DoF and Antenna Range: Similar to the analyses for model 1, the number of antennas plays a key role to implement alignment, while the feasibility conditions are not solved in general. The antennas could have different balance between BS side and MS side to achieve alignment.

The aim of this work is exploit interference alignment with limited provision of antennas at both BS side and MS side with a balance. For all the five approaches, all the antenna configurations are listed in Table IV, in which the notations of 'A', 'B', 'C', 'D' and 'E' denote the five approaches in sequence.

In summary, as shown in Table IV, approach 'B' and 'E' need a large number of antennas for BS nodes. Compared model 1 in Table I, the antenna requirement is greatly reduced, especially for MS nodes.

Approach	Minimum BS Antenna.	Minimum MS Antenna
A	Md	$2Md+d$
B	$2M^2d+Md$	Md
C	$2Md$	$4Md$
D	$(M+2)d$	$2\frac{(M-1)}{M}(M+2)d$ $+d/M$
E	$2M^2d$ $+(M/K)d$	$2Md$

TABLE IV
MINIMUM ANTENNA USAGE FOR BSS AND MSS IN ALL APPROACHES IN MODEL 2

2) CSI Overhead: Similar to the analyses for model 1, the proposed interference alignment approaches require all the BS nodes and MS nodes to have certain knowledge of channel state information (CSI).

The aim of this work is to compare the CSI requirements for the network in different approaches. For the above five approaches, all the CSI configurations are listed in Table V. The notations from 'A' to 'E' denote the five approaches in sequence. Other settings are also the same as in model 1.

Approach	required CSI at k-th BS		
	Source	Content	Quantity
A	all intra-cell MSs	$\mathbf{U}_{k:m}^{\dagger}\mathbf{H}_k^{k:m}$	M
B	adjacent inter-cell MSs	$\mathbf{\Psi}_{j:n}^{\dagger}\mathbf{H}_k^{j:n}$	$2M$
C	all intra-cell MSs	$\mathbf{G}_{k:m}\mathbf{H}_k^{k:m}$	M
D	all intra-cell MSs adjacent inter-cell MSs	$\mathbf{U}_{k:m}^{\dagger}\mathbf{H}_k^{k:m}$,$\mathbf{\Omega}_k^j$	M,2
E	adjacent inter-cell MSs	$\mathbf{H}_k^{j:m}$	$2M$ (excl. backhaul)

Approach	required CSI at m-th MS in k-th cell		
	Source	Content	Quantity
A	adjacent inter-cell BSs	$\mathbf{H}_j^{k:m}\mathbf{\Phi}_j$	2
B	intra-cell BS	$\mathbf{H}_k^{k:m}\mathbf{V}_{k:n}$	$(M-1)$
C	adjacent inter-cell BSs	$\mathbf{H}_j^{k:m}$	2
D	adjacent inter-cell BSs	$\mathbf{H}_j^{k:m}$	2 (excl. conferencing)
E	intra-cell BS	$\mathbf{H}_k^{k:m}\mathbf{V}_{k:n}$,$\mathbf{\Theta}^{k:m}$	$(M-1)$,1

TABLE V
CSI FOR BSS AND MSS IN ALL APPROACHES IN MODEL 2

In summary, as shown in Table V, approach 'B' and 'E' need a large amount of CSI. Compared with Table II of model 1, the CSI requirement is lowered in general. While the requirements for inter-cell CSI or intra-cell CSI are still the same for corresponding nodes.

3) Computational Complexity: Similar to the analyses for model 1, all the nodes need to calculate their coding matrices or filters with obtained CSI. The calculations use different operations, and are commonly measured by the metric of computational complexity.

The aim of this work is to compare the computational complexities for the network using different approaches. For the above five approaches, all the complexity configurations are listed in Table VI. The notations from 'A' to 'E' denote the five approaches in sequence. Other settings are also the same as model 1.

In summary, as shown in Table VI, approach 'D' and 'E' need a large amount of computational complexities. Compared with model 1 in Table III, however the expended complexity is reduced greatly.

V. BASIC DESIGN AND ANALYSIS OF MODEL 3

This section looks into model 3 as shown in Fig. 3, equation (3) and (4). Similar to model 2, another Wyner-type model is studied here. It has only one interference link between the BS and MSs belonging to two neighboring cells, in a cascaded fashion in the cyclic network. It could be also referred as the Z-interference channel (ZIC) or cylic interference channel [31], [25]. Previous researches only focus on the capacity regions by using Han-Kobayashi schemes. However in this work, the focus is on the DoF structure of interference in this cellular network. Similar to model 1 and model 2, five approaches are proposed to implement the alignment as following.

Clarification: the notations are similar to the analyses for model 1 and model 2. Some symbols are reused so long as they do not cause any confusion. In the expression of the design process referring to an arbitrary BS or MS in a set, the variable index may change between successive steps accordingly in the discussion. They may change in corresponding tables as well.

Approach	expended Complexity at k-th BS		
	Target	Operation	Scale
A	$\tilde{\mathbf{V}}_{k:m}$	matrix inverse	$Md \times Md$
B	$\mathbf{V}_{k:m}$	null space	$N_t \times Md$
C	$\mathbf{V}_{k:m}$	matrix inverse	$2Md \times N_t$
D	$\mathbf{V}_{k:m}$	matrix inverse	$(M+2)d \times N_t$
E	$\mathbf{V}_{k:m}, \mathbf{\Theta}^{k:m}$	null space	$(KMN_r + KN_t) \times Md$

Approach	expended Complexity at m-th MS in k-th cell		
	Target	Operation	Scale
A	$\mathbf{U}_{k:m}$	null space	$N_r \times d$
B	$\tilde{\mathbf{U}}_{k:m}$	null space	$Md \times d$
C	$\mathbf{G}_{k:m}$	matrix inverse	$N_r \times 2N_t$
D	$\mathbf{U}_{k:m}$,$\mathbf{\Omega}_j^k$	null space	$(2N_t + MN_r) \times d$
E	$\mathbf{U}_{k:m}$	null space	$N_r \times d$

TABLE VI
COMPLEXITY FOR BSS AND MSS IN ALL APPROACHES IN MODEL 2

A. Approach on Transmitter Side with Cascaded Coder

This approach is similar to the design of [14] as used in model 1 and model 2. Each BS uses a cascaded precoder to zero-forcing ICI, and then deal with its own IUI. The whole process takes four steps as following:

Step 1: Choose an auxiliary intermediate precoder $\mathbf{\Phi}_k \in \mathbb{C}^{N_t \times (M \cdot d)}$ at k-th BS (transmitter), and a second precoder $\tilde{\mathbf{V}}_{k:m} \in \mathbb{C}^{(M \cdot d) \times d}$ preceding the first chosen precoder. Then the actual precoder $\mathbf{V}_{k:m}$ is composed of:

$$\mathbf{V}_{k:m} = \mathbf{\Phi}_k \tilde{\mathbf{V}}_{k:m} \quad m \in \mathcal{M}, k \in \mathcal{K} \tag{43}$$

(Notice the index refers to all equal nodes.)

Step 2: When the first precoder $\mathbf{\Phi}_j$ is randomly picked, to enable zero-forcing the ICI from the only one adjacent cell, all the M° cell-edge MSs in k-th cell should determine $\mathbf{U}_{k:m^\circ}$ to satisfy the following conditions (index changed):

$$\mathbf{U}_{k:m^\circ}^\dagger \mathbf{H}_{k+1}^{k:m^\circ} \mathbf{\Phi}_{k+1} = \mathbf{0} \quad m^\circ \in \mathcal{M}^\circ \tag{44}$$

To be feasible to find $\mathbf{U}_{k:m^\circ}$, the dimensions should satisfy $N_r^\circ \geq Md + d$ for cell-edge users, where N_r° is the number of receive antennas of any MS in the edge set $\mathcal{M}^\circ$. While for cell-interior users, the receive filters $\mathbf{U}_{k:m^\star}$ for $M^\star$ cell-interior MSs in k-th cell could be randomly generated. So that it's only required the dimensions should satisfy $N_r^\star \geq d$, where $N_r^\star$ is the number of receive antennas of any MS in the interior set $\mathcal{M}^\star$. Compared with analyses for model 1 and model 2, the requirements for antennas are greatly loosened.

Step 3: Now observe each $\mathbf{\Phi}_k$ again, there're M° zero-forcing conditions to satisfy (notice change of index):

$$\begin{bmatrix} \vdots \\ \mathbf{U}_{k-1:m^\circ}^\dagger \mathbf{H}_k^{k-1:m^\circ} \\ \vdots \end{bmatrix} \mathbf{\Phi}_k = \mathbf{0} \quad m^\circ \in \mathcal{M}^\circ \tag{45}$$

Remark 11: check the condition (45). Normally it is feasible to find $\mathbf{\Phi}_k$ only when $N_t \geq Md + M^\circ d$. However, since (44) already guarantees this condition, it is only required that $N_t \geq Md$ in this specific design process. So this process naturally contains an *implicit* and *inherent* alignment.

Step 4: Then each k-th BS knows its equivalent downlink channel $\mathbf{U}_{k:m}\mathbf{H}_k^{k:m}\mathbf{\Phi}_k$ from each intra-cell MS. It forms zero-forcing transmit streams eliminating IUI, without knowing the actual interfering streams. The second precoder matrix is obtained by an inverse operation:

$$\begin{bmatrix} \tilde{\mathbf{V}}_{k:1} & \tilde{\mathbf{V}}_{k:2} & \cdots & \tilde{\mathbf{V}}_{k:M} \end{bmatrix} = \begin{bmatrix} \mathbf{U}_{k:1}^\dagger \mathbf{H}_k^{k:1} \mathbf{\Phi}_k \\ \mathbf{U}_{k:2}^\dagger \mathbf{H}_k^{k:2} \mathbf{\Phi}_k \\ \vdots \\ \mathbf{U}_{k:M}^\dagger \mathbf{H}_k^{k:M} \mathbf{\Phi}_k \end{bmatrix}^{-1} \tag{46}$$

In summary, the four steps determine intermediate precoders, receive filters, and second precoders in sequence. Alignment is implicitly contained in step 3. Compared with model 1 and model 2, it is evident that less antennas are used to implement alignment, because there is only one adjacent interfering path for each cell and only cell-edge users are involved and affected.

B. Approach on Receiver Side with Cascaded Coder: I

This approach is proposed as a dual solution of the above approach on transmitter side. Set the cascaded coders for the cell-edge users on the receiver side. Then the whole process takes the following four steps:

Step 1: Choose an auxiliary or intermediate receive filter matrix $\mathbf{\Psi}_{k:m^\circ} \in \mathbb{C}^{N_r^\circ \times Md}$ at the m°-th cell-edge MS in k-th cell, and a second receive filter $\tilde{\mathbf{U}}_{k:m^\circ} \in \mathbb{C}^{Md \times d}$ preceding the first chosen receive filter. Then the actual receive filter $\mathbf{U}_{k:m^\circ}$ is composed of:

$$\mathbf{U}_{k:m^\circ} = \mathbf{\Psi}_{k:m^\circ} \tilde{\mathbf{U}}_{k:m^\circ} \quad m^\circ \in \mathcal{M}^\circ, k \in \mathcal{K} \tag{47}$$

While for cell-interior users, any $m^\star$-th MS in the k-th cell has a complete receive filter $\mathbf{U}_{k:m^\star}, m^\star \in \mathcal{M}^\star$.

Step 2: When every first receive filter $\mathbf{\Psi}_{j:n^\circ}$ is randomly picked, to enable zero-forcing ICI, the k-th BS should determine $\mathbf{V}_{k:m}, m \in \mathcal{M}$ which satisfies the condition:

$$\begin{bmatrix} \vdots \\ \mathbf{\Psi}_{k-1:n^\circ}^\dagger \mathbf{H}_k^{k-1:n^\circ} \\ \vdots \end{bmatrix} [\mathbf{V}_{k:1} \ \mathbf{V}_{k:2} \ \cdots \ \mathbf{V}_{k:M}] = \mathbf{0} \quad n \in \mathcal{M}^\circ \tag{48}$$

To be feasible to determine $[\mathbf{V}_{k:1} \ \mathbf{V}_{k:2} \ \cdots \ \mathbf{V}_{k:M}]$, the dimensions should satisfy $N_t \geq M^\circ Md + Md$. Compared with model 1 and model 2, the requirement for antennas is greatly reduced.

Step 3: Now observe each $\mathbf{\Psi}_{k:m^\circ}, m^\circ \in \mathcal{M}^\circ$ again, notice there're M° zero-forcing conditions to satisfy:

$$\mathbf{\Psi}_{k:m^\circ}^\dagger \underbrace{[\cdots \ \mathbf{H}_{k+1}^{k:m} \mathbf{V}_{k+1:n} \ \cdots]}_{n \in \mathcal{M}} = \mathbf{0} \quad m^\circ \in \mathcal{M}^\circ \tag{49}$$

Remark 12: Check the condition of (49). Notice in general it is only feasible to find $\mathbf{\Psi}_{k:m^\circ}$ when the dimensions satisfy $N_r^\circ \geq Md + Md$. However, since (48) already guarantees the condition, it is only required that $N_r^\circ \geq Md$ in this specific design process. So this process naturally contains an *implicit* and *inherent* alignment.

Step 4: Then each cell-edge MS in the k-th cell knows its equivalent channel $\mathbf{\Psi}_{k:m^\circ}^\dagger \mathbf{H}_k^{k:m^\circ} \mathbf{V}_{k:n}, m^\circ \in \mathcal{M}^\circ, n \in \mathcal{M}$. Also each cell-interior MS in the k-th cell knows its equivalent channel $\mathbf{H}_k^{k:m^\star} \mathbf{V}_{k:n}, m^\star \in \mathcal{M}^\star, n \in \mathcal{M}$. Also they do not know the actual interfering beams, they could form zero-forcing receive filters to eliminate IUI. The second receive filters $\tilde{\mathbf{U}}_{k:m^\circ}$ and $\mathbf{U}_{k:m^\star}$ for cell-edge and cell-interior users respectively are determined by an operation to find the null space:

$$\begin{aligned} \tilde{\mathbf{U}}_{k:m^\circ}^\dagger \left[\underbrace{\cdots \ \mathbf{\Psi}_{k:m^\circ}^\dagger \mathbf{H}_k^{k:m^\circ} \mathbf{V}_{k:n} \ \cdots}_{n \in \mathcal{M} \setminus \{m^\circ\}} \right] &= \mathbf{0} \\ \mathbf{U}_{k:m^\star}^\dagger \left[\underbrace{\cdots \ \mathbf{H}_k^{k:m^\star} \mathbf{V}_{k:n} \ \cdots}_{n \in \mathcal{M} \setminus \{m^\star\}} \right] &= \mathbf{0} \end{aligned} \tag{50}$$

To be feasible to determine $\mathbf{U}_{k:m^\star}$, the dimensions should satisfy $N_r^\star \geq Md$.

In summary, the four steps determine intermediate receive filters, precoders, second receive filters in sequence. Alignment is implicitly contained in step 3. Compared with model 1 and model 2, the usage of antennas is evidently reduced because the loose connectivity only between adjacent BS and cell-edge MSs.

C. Approach on Receiver Side with Cascaded Coder: II

This approach is similar to the design of [15]. Each cell-interior MS uses a cascaded receive filter to align ICI from only one adjacent cell, and deal with ICI and IUI in its own cell. The whole process takes four steps as following:

Step 1: For each m°-th ($m^\circ \in \mathcal{M}^\circ$) cell-edge MS in k-th cell, the receive filter $\mathbf{U}_{k:m^\circ}$ is defined as two cascaded filter matrices:

$$\begin{aligned} &\mathbf{U}_{k:m^\circ} = \mathbf{G}_{k:m^\circ}^\dagger \Lambda_{\mathcal{K}:m^\circ} \\ &\mathbf{G}_{k:m^\circ} = \mathbf{H}_{k+1}^{k:m^\circ -1} \\ &\text{So that} \ \ \mathbf{G}_{k:m^\circ} \in \mathbb{C}^{N_t \times N_r^\circ} \end{aligned} \tag{51}$$

$\mathbf{G}_{k:m^\circ}$ is set to make all ICI from the neighboring cell aligned together. While $\Lambda_{\mathcal{K}:m^\circ}$ is a common filter set to be the same for all cells in the network.

To be feasible to determine $\mathbf{G}_{k:m^\circ}$ by the inverse operation, the dimensions should satisfy $N_r^\circ \geq N_t$. While for each $m^\star$-th ($m^\star \in \mathcal{M}^\star$) cell-interior MS in k-th cell, it is only required the dimensions should satisfy $N_r^\star \geq d$. Compared with model 1 and model 2, it is obvious that these conditions are greatly loosened to save a number of antennas.

Step 2: Since the common receive filter $\Lambda_{\mathcal{K}:m^\circ} \in \mathbb{C}^{N_t \times d}$ is set to be the same for all cells of $\mathcal{K}$, the output stream of (4) is presented as following:

$$\begin{aligned}\Lambda_{\mathcal{K}:m^\circ}^\dagger \mathbf{G}_{k:m^\circ} \mathbf{y}_{k:m^\circ} = \\ \Lambda_{\mathcal{K}:m^\circ}^\dagger \mathbf{G}_{k:m^\circ} \mathbf{H}_k^{k:m^\circ} \mathbf{V}_{k:m^\circ} \mathbf{x}_{k:m^\circ} \\ + \sum_{n \neq m^\circ}^{n \in \mathcal{M}} \Lambda_{\mathcal{K}:m^\circ}^\dagger \mathbf{G}_{k:m^\circ} \mathbf{H}_k^{k:m^\circ} \mathbf{V}_{k:n} \mathbf{x}_{k:n} \\ + \sum_{n \in \mathcal{M}} \Lambda_{\mathcal{K}:m^\circ}^\dagger \mathbf{V}_{k+1:n} \mathbf{x}_{k+1:n}\end{aligned} \tag{52}$$

To eliminate ICI and IUI terms in equation (52) respectively, the zero-forcing conditions should be set as:

$$\begin{aligned}\Lambda_{\mathcal{K}:m^\circ}^\dagger \mathbf{G}_{k:m^\circ} \mathbf{H}_k^{k:m^\circ} \mathbf{V}_{k:n} = \mathbf{0} \quad n \in \mathcal{M} \backslash \{m^\circ\} \\ \Lambda_{\mathcal{K}:m}^\dagger \mathbf{V}_{k+1:n} = \mathbf{0} \quad n \in \mathcal{M}\end{aligned} \tag{53}$$

Compared with model 1 and model 2, the condition is loosened a lot.

While for each cell-interior $m^\star$-th ($m^\star \in \mathcal{M}^\star$) MS in k-th cell, the receiver filter $\mathbf{U}_{k:m^\star}$ is in a complete form and randomly chosen.

Step 3: Then observe from the k-th BS to choose the precoder $[\cdots \ \mathbf{V}_{k:m} \ \cdots]$. The zero-forcing conditions in equation (53) are equivalently presented with new indices in the following expressions:

$$\begin{aligned}\mathbf{U}_{k:n}^\dagger \mathbf{H}_k^{k:n} \mathbf{V}_{k:m} = \mathbf{0} \quad n \in \mathcal{M}^\star \backslash \{m\}, m \in \mathcal{M} \\ \Lambda_{\mathcal{K}:n}^\dagger \mathbf{G}_{k:n} \mathbf{H}_k^{k:n} \mathbf{V}_{k:m} = \mathbf{0} \quad n \in \mathcal{M}^\circ, m \in \mathcal{M}^\star \\ \Lambda_{\mathcal{K}:n}^\dagger \mathbf{G}_{k:n} \mathbf{H}_k^{k:n} \mathbf{V}_{k:m} = \mathbf{0} \quad n \in \mathcal{M}^\circ \backslash \{m\}, m \in \mathcal{M}^\circ \\ \Lambda_{\mathcal{K}:n}^\dagger \mathbf{V}_{k:m} = \mathbf{0} \quad n \in \mathcal{M}^\circ, m \in \mathcal{M}\end{aligned} \tag{54}$$

The last condition in equation (54) is due to the ICI to the adjacent cell. Compared with model 1 and model 2, notice that the conditions are different for cell-edge users and cell-interior users.

Step 4: So for each k-th BS, the precoder should be determined by only one inverse operation:

$$\begin{aligned}[\underbrace{\cdots \mathbf{V}_{k:m^\star}}_{m^\star \in \mathcal{M}^\star} \underbrace{\cdots\cdots \mathbf{V}_{k:m^\circ} \cdots}_{m^\circ \in \mathcal{M}^\circ}] = \text{The first } Md \text{ columns of} \\ \begin{bmatrix} \vdots \\ \mathbf{U}_{k:m^\star}^\dagger \mathbf{H}_k^{k:m^\star} \\ \vdots \end{bmatrix} m^\star \in \mathcal{M}^\star \\ \begin{bmatrix} \vdots \\ \Lambda_{\mathcal{K}:m^\circ}^\dagger \mathbf{G}_{k:m^\circ} \mathbf{H}_k^{k:m^\circ} \\ \vdots \end{bmatrix} m^\circ \in \mathcal{M}^\circ \\ \begin{bmatrix} \vdots \\ \Lambda_{\mathcal{K}:n}^\dagger \\ \vdots \end{bmatrix} n \in \mathcal{M}^\circ \end{bmatrix}^{-1}\end{aligned} \tag{55}$$

Check that $[\underbrace{\cdots \mathbf{V}_{k:m^\star}}_{m^\star \in \mathcal{M}^\star} \underbrace{\cdots\cdots \mathbf{V}_{k:m^\circ} \cdots}_{m^\circ \in \mathcal{M}^\circ}]$ indeed satisfies the conditions in (54).

Remark 13: To be feasible to obtain $[\underbrace{\cdots \mathbf{V}_{k:m^\star}}_{m^\star\in\mathcal{M}^\star} \underbrace{\cdots\cdots \mathbf{V}_{k:m^\circ}}_{m^\circ\in\mathcal{M}^\circ} \cdots]$ by an inverse operation, the dimensions should satisfy $N_t \geq Md + M^\circ d$. While in general cases, it is required that $N_t \geq Md + Md$ for the BS to handle interferences to the adjacent cell. So this process naturally contains an *implicit* and *inherent* alignment.

In summary, the four steps determine receive filters, precoders and second receive filters in sequence. Alignment is explicitly presented in step 1. Compared with model 1 and model 2, less antennas are required to implement alignment because of the loose connectivity.

D. Approach from Receiver Side with Direct Interplay

This approach is similar to the design of [18]. The alignment is jointly implemented on both BS(transmitter) side and MS(receiver) side via intricate and meticulous interplays and cooperations. The whole process takes two steps as following:

Step 1: Regarding channels from the $(k+1)$-th BS to all cell-edge MSs in the k-th cell, the equivalent receive filtered channel subspaces are set to be equal to a random predetermined reference subspace:

$$\cdots = \mathbf{U}_{k:m^\circ}^\dagger \mathbf{H}_{k+1}^{k:m^\circ} = \cdots = (\mathbf{\Omega}_{k+1}^k)^\dagger \qquad m^\circ \in \mathcal{M}^\circ \tag{56}$$

Remark 14: Notice that the step of (56) is an *explicit* alignment of ICI from the $(k+1)$-th BS to all cell-edge MSs in the adjacent cell.

Observe from all cell-edge MSs in the k-th cell, (index changed) to satisfy the condition (56), $\mathbf{U}_{k:m^\circ}$ and $\mathbf{\Omega}_{k+1}^k$ could be found by solving the following null space problem:

$$\begin{bmatrix} (\mathbf{\Omega}_{k+1}^k)^\dagger & \cdots & \mathbf{U}_{k:m^\circ}^\dagger & \cdots \end{bmatrix} \bullet \begin{bmatrix} \mathbf{I}_{N_t} & \cdots & \mathbf{I}_{N_t} & \\ \ddots & & & \\ & -\mathbf{H}_{k+1}^{k:m^\circ} & & \\ & & \ddots & \end{bmatrix} = \mathbf{0} \tag{57}$$

To be feasible to obtain $\mathbf{U}_{k:m^\circ}$ and $\mathbf{\Omega}_{k+1}^k$ via a null space operation, the dimensions should satisfy $N_t + M^\circ N_r^\circ \geq MN_t + d$. While for cell-interior MSs, it is only required the dimensions satisfy $N_r^\star \geq d$. Compared with model 1 and model 2, the conditions are greatly loosened to save a number of antennas.

Step 2: Thus for the k-th BS, the precoders are determined by the following inverse operation to eliminate both IUI and ICI:

$$[\underbrace{\cdots \mathbf{V}_{k:m^\star}}_{m^\star\in\mathcal{M}^\star} \underbrace{\cdots\cdots \mathbf{V}_{k:m^\circ}}_{m^\circ\in\mathcal{M}^\circ} \cdots] = \text{The first } Md \text{ columns of} \begin{bmatrix} \vdots \\ \mathbf{U}_{k:m^\star}^\dagger \mathbf{H}_k^{k:m^\star} \\ \vdots \end{bmatrix} m \in \mathcal{M}^\star \\ \begin{bmatrix} \vdots \\ \mathbf{U}_{k:m^\circ}^\dagger \mathbf{H}_k^{k:m^\circ} \\ \vdots \end{bmatrix} m^\circ \in \mathcal{M}^\circ \\ (\mathbf{\Omega}_k^{k-1})^\dagger \Bigg]^{-1} \tag{58}$$

To be feasible to obtain $[\underbrace{\cdots \mathbf{V}_{k:m^\star}}_{m^\star\in\mathcal{M}^\star} \underbrace{\cdots\cdots \mathbf{V}_{k:m^\circ}}_{m^\circ\in\mathcal{M}^\circ} \cdots]$ via the inverse operation, the dimensions should satisfy $N_t \geq Md + d$. Compared with model 1 and model 2, the condition is loosened.

Check the equation (58) and find that $[\underbrace{\cdots \mathbf{V}_{k:m^\star}}_{m^\star\in\mathcal{M}^\star} \underbrace{\cdots\cdots \mathbf{V}_{k:m^\circ}}_{m^\circ\in\mathcal{M}^\circ} \cdots]$ indeed eliminate the IUI in the cell and ICI to the adjacent cell.

In summary, the two steps determine receive filters, aligned subspace and precoders in sequence. Alignment is explicitly and implicitly implemented on the MS side and BS side. Compared with model 1 and model 2, the requirement for antennas is greatly reduced because of the loose connectivity.

E. Approach from Transmitter Side with Direct Interplay

This approach is proposed as a dual solution of the above approach on receiver side. It implements the alignment on the BS side. The whole process takes the following two steps:

Step 1: Regarding channels from the $(k+1)$-th BS to all cell-edge MSs in k-th cell, the equivalent precoded channel subspaces are set to be equal to a random predetermined reference subspace:

$$\mathbf{H}_{k+1}^{k:m^\circ}[\mathbf{V}_{k+1:1}\cdots\mathbf{V}_{k+1:M}] = \mathbf{\Theta}^{k:m^\circ} \qquad m^\circ \in \mathcal{M}^\circ \tag{59}$$

Remark 15: Notice the step of (59) is *not* an alignment.

Observe from the side of all BSs, (index changed) to satisfy the condition (59), $[\mathbf{V}_{k:1}\cdots\mathbf{V}_{k:M}]$ and $\mathbf{\Theta}^{k:m^\circ}$ could be found by solving the following null space problem:

$$\begin{bmatrix} \mathbf{I}_{N_r^\circ} & & -\mathbf{H}_2^{1:m^\circ} \\ & \ddots & & \ddots \end{bmatrix} \Big\} m^\circ \in \mathcal{M}^\circ$$
$$\begin{bmatrix} \mathbf{I}_{N_r^\circ} & & -\mathbf{H}_{k+1}^{k:m^\circ} \\ & \ddots & & \ddots \end{bmatrix} \Big\} m^\circ \in \mathcal{M}^\circ$$
$$\begin{bmatrix} \mathbf{I}_{N_r^\circ} & & -\mathbf{H}_1^{K:m^\circ} \\ & \ddots & & \ddots \end{bmatrix} \Big\} m^\circ \in \mathcal{M}^\circ$$
$$\bullet \begin{bmatrix} \vdots \\ \mathbf{\Theta}^{k:m^\circ} \\ \vdots \end{bmatrix} \Big\} k \in \mathcal{K} \Big\} m^\circ \in \mathcal{M}^\circ \quad \bullet \begin{bmatrix} \vdots \\ [\mathbf{V}_{k:1}\cdots\mathbf{V}_{k:M}] \\ \vdots \end{bmatrix} \Big\} k \in \mathcal{K} = \mathbf{0} \tag{60}$$

To be feasible to obtain $[\mathbf{V}_{k:1}\cdots\mathbf{V}_{k:M}]$ and $\mathbf{\Theta}^{k:m^\circ}$ via a null space operation, the dimensions should follow $KM^\circ N_r^\circ + KN_t \geq KM^\circ N_r^\circ + Md$. Obviously this actual condition $KN_t \geq Md$ is a very loose contraint because the cell-edge MSs have enough space of receive antennas. So for the BS, it is required the dimensions satisfy the basic constraint $N_t \geq Md$.

Step 2: Thus for the m-th MS (cell-edge and cell-interior respectively) in k-th cell, its receive filter is determined via a null space operation to eliminate both IUI and ICI:

$$\begin{aligned} \mathbf{U}_{k:m^\circ}^\dagger \begin{bmatrix} \mathbf{H}_k^{k:m^\circ} \big[\underbrace{\cdots\ \mathbf{V}_{k:n}\ \cdots}_{n\in\mathcal{M}\setminus\{m^\circ\}}\big] & \mathbf{\Theta}^{k:m^\circ} \end{bmatrix} &= \mathbf{0} \quad m^\circ \in \mathcal{M}^\circ \\ \mathbf{U}_{k:m^\star}^\dagger\ \mathbf{H}_k^{k:m^\star}\big[\underbrace{\cdots\ \mathbf{V}_{k:n}\ \cdots}_{n\in\mathcal{M}\setminus\{m^\star\}}\big] &= \mathbf{0} \quad m^\star \in \mathcal{M}^\star \end{aligned} \tag{61}$$

To be feasible to obtain $\mathbf{U}_{k:m^\circ}$ for the cell-edge MS, the dimension should follow $N_r^\circ \geq (M-1)d + Md + d$. For the cell-interior MS to obtain $\mathbf{U}_{k:m^\star}$, the dimension should follow $N_r^\star \geq (M-1)d + d$. It is easy to check the conditions of (61) directly eliminates both IUI and ICI.

In summary, the two steps determine precoders, aligned subspaces, and receive filters in sequence. Alignment is not necessary. Compared with model 1 and model 2, the requirement for antennas is only reduced for cell-interior MSs.

Approach	Minimum BS Antenna.	Minimum MS Antenna $(N_r^\star, N_r^\circ)$
A	Md	$(d, Md+d)$
B	$(M^\circ+1)Md$	(Md, Md)
C	$Md+M^\circ d$	$(d, Md+M^\circ d)$
D	$(M+1)d$	$(d,\ (M^2/M^\circ)d)$
E	Md	$(Md, 2Md)$

TABLE VII
MINIMUM ANTENNA USAGE FOR BSS AND MSS IN ALL APPROACHES IN MODEL 3

F. Comparison of System Conditions

Similar to the analyses for model 1 and model 2, system conditions are listed and compared for all the proposed five approaches of downlink interference alignment in a Wyner-type cellular network with only one adjacent link for each cell. Three aspects are investigated including the usage of antennas, required CSI, and computational complexity. Moreover, in this case, the design deliberately considers distinguishing between cell-interior and cell-edge users corresponding to the realistic settings of the network [6], and actually it benefits the obtained DoF and saves part of the CSI overhead.

1) DoF and Antenna Range: Similar to the analyses for model 1 and model 2, the number of antennas determine the achievable DoF for all the nodes. The aim of this work is to exploit alignment with limited antennas in the specified Wyner-type network. For all the five approaches, all the antenna configurations are listed in Table VII, in which the notations of 'A', 'B', 'C', 'D' and 'E' denote the five approaches in sequence.

In summary, as shown in Table VII, approach 'B' needs a large number of antennas for BS nodes. Compared with model 2 in Table IV, the antenna requirement is greatly reduced. Cell-interior MSs generally need less antennas than cell-edge MSs.

2) CSI Overhead: Similar to the analyses in model 1 and model 2, the proposed alignment approaches require all the BS nodes and MS nodes to have different knowledge of channel state information (CSI). The aim of this work is to compare the CSI requirements of different approaches. For the five approaches, all the CSI configurations are listed in Table VIII. The notations from 'A' to 'E' denote the five approaches in sequence. Other settings are the same as model 1 and model 2.

Approach	required CSI at k-th BS from Interior and Edge MSs $(m^\star, m^\circ)$		
	Source	Content	Quantity
A	all intra-cell MSs	$\mathbf{U}_{k:m}^\dagger \mathbf{H}_k^{k:m}$	M
B	adjacent inter-cell MSs	$(/, \mathbf{\Psi}_{k-1:n}^\dagger \mathbf{H}_k^{k-1:n})$	M°
C	all intra-cell MSs	$(\mathbf{U}_{k:m^\star}^\dagger \mathbf{H}_k^{k:m^\star}, \mathbf{G}_{k:m^\circ} \mathbf{H}_k^{k:m^\circ})$	$(M^\star, M^\circ)$
D	all intra-cell MSs adjacent inter-cell MSs	$(\mathbf{U}_{k:m^\star}^\dagger \mathbf{H}_k^{k:m^\star}, \mathbf{U}_{k:m^\circ}^\dagger \mathbf{H}_k^{k:m^\circ}), \mathbf{\Omega}_k^{k-1}$	$(M^\star, M^\circ), 1$
E	adjacent inter-cell MSs	$(/, \mathbf{H}_k^{k-1:m^\circ})$	M°(excl. backhaul)
Approach	required CSI at m-th MS in k-th cell $(m^\star, m^\circ)$		
	Source	Content	Quantity
A	adjacent inter-cell BS	$(/, \mathbf{H}_{K+1}^{k:m^\circ} \mathbf{\Phi}_{K+1})$	1
B	intra-cell BS	$(\mathbf{H}_k^{k:m^\star} \mathbf{V}_{k:n}, \mathbf{\Psi}_{k:m^\circ}^\dagger \mathbf{H}_k^{k:m^\circ} \mathbf{V}_{k:n})$	$(M-1, M-1)$
C	adjacent inter-cell BS	$(/, \mathbf{H}_{k+1}^{k:m^\circ})$	1
D	adjacent inter-cell BS	$\mathbf{H}_{k+1}^{k:m^\circ}$	1(excl. conferencing)
E	intra-cell BS	$(\mathbf{H}_k^{k:m^\star} \mathbf{V}_{k:n}, \mathbf{H}_k^{k:m^\circ} \mathbf{V}_{k:n}), \mathbf{\Theta}^{k:m^\circ}$	$(M-1, M-1), 1$

TABLE VIII
CSI FOR BSS AND MSS IN ALL APPROACHES IN MODEL 3

In summary, as shown in Table VIII, approach 'B' and 'E' need a large amount of CSI. Compared with model 2 in Table V, the CSI requirement is lowered in general. Each BS require less CSI from cell-interior MSs than from cell-edge MSs. While cell-interior MSs require less CSI than cell-edge MSs do.

3) Computational Complexity: Similar to the analyses for model 1 and model 2, all the nodes need to calculate coding matrices or filters with obtained channel knowledge. The calculations apply different operations and are universally measured

by the metric of computational complexity. The aim of this work is to compare the computational complexities for the proposed approaches. For all the five approaches, all the complexity configurations are listed in Table IX. The notations from 'A' to 'E' denote the five approaches in sequence. Other settings are the same as model 1 and model 2.

Approach	expended Complexity at k-th BS		
	Target	Operation	Scale
A	$\tilde{\mathbf{V}}_{k:m}$	matrix inverse	$Md \times Md$
B	$\mathbf{V}_{k:m}$	null space	$N_t \times Md$
C	$\mathbf{V}_{k:m}$	matrix inverse	$(M+M^{\circ})d \times N_t$
D	$\mathbf{V}_{k:m}$	matrix inverse	$(M+1)d \times N_t$
E	$\mathbf{V}_{k:m}, \mathbf{\Theta}^{k:m^{\circ}}$	null space	$(KM^{\circ}N_r^{\circ} + KN_t) \times Md$

Approach	expended Complexity at m-th MS in k-th cell $(m^{\star}, m^{\circ})$		
	Target	Operation	Scale
A	$(/, \tilde{\mathbf{U}}_{k:m^{\circ}})$	null space	$N_r^{\circ} \times d$
B	$(\mathbf{U}_{k:m^{\star}}, \tilde{\mathbf{U}}_{k:m^{\circ}})$	null space	$(N_r^{\star} \times d, N_r^{\circ} \times d)$
C	$(/, \mathbf{G}_{k:m^{\circ}})$	matrix inverse	$N_r^0 \times N_t$
D	$(/, (\mathbf{U}_{k:m^{\circ}}, \mathbf{\Omega}_j^k))$	null space	$(N_t + M^{\circ}N_r^{\circ}) \times d$
E	$(\mathbf{U}_{k:m^{\star}}, \mathbf{U}_{k:m^{\circ}})$	null space	$(N_r^{\star} \times d, N_r^{\circ} \times d)$

TABLE IX
COMPLEXITY FOR BSS AND MSS IN ALL APPROACHES IN MODEL 3

In summary, as shown in Table IX, approach 'D' and 'E' need a large amount of computational complexities. Compared with model 2 in Table VI, the expended complexities are reduced. Cell-interior MSs require less complexities than cell-edge MSs.

VI. ADVANCED DESIGN AND ANALYSIS OF PRAGMATIC MODELS

The previous sections 5.3, 5.4 and 5.5 discuss comprehensive and basic approaches for the three models. However, they are not as perfect solutions as real cellular networks desire. These basic solutions need to be further specialized and enhanced.

This section crystalizes the designs and analyses in previous investigations and looks into pragmatic models which are fit to current cellular systems. Advanced schemes are proposed to obtain better performance for these typical models in the discussion.

A. Motivations, Models, and Strategies

In previous sections, for model 1, model 2, and model 3, elaborate designs and analyses are proposed, which are non-trivial extensions from two-cell scenarios and schemes as in [14], [15], [18] to general multi-cell scenarios and schemes. However, new issues come out in different angles. First, all the approaches applied for each model mainly implement alignment on either the BS side or on the MS side. If the alignment happens on both sides within certain antenna range, there is potential advantage for the achievable DoF while the implementation is not explicit. Second, all the approaches only consider alignment between IUI and ICI as the conventional design, while if there are more than two cells, the alignment between ICI and ICI from different interfering cells are potentially exploitable. Third, all the approaches require cooperations of BSs or MSs in all cells with a large amount of unrealistic global CSI. Actually it could be improved in realistic settings by introducing a sequential process to construct alignment in a more local way.

Proper models are needed in order to be fit to the general framework of cellular networks. Model 1, model 2 and model 3 are comprehensively studied in previous sections. While in the following part, only model 2 and model 3 are considered. The reasons are as following. Model 1 is a full connected K-cell network. When K is large or the network is large, the connectivity is not realistic due to path loss. Furthermore this model is not tractable to analyze or design because it needs many antennas and CSI exchange. Model 2 is a cyclic Wyner network with two adjacent links for each cell. It represents a usual scenario of cellular networks, which has multiple cells and appropriate interfering links between adjacent cells. Model 3 is a cyclic Wyner network with one adjacent link for each cell and only cell-edge users are interfered. This model is simple but typical. In the following discussion for model 2 and model 3, all cell indices from 1 to K are in the set $\mathcal{K}$ in a circular manner, i.e. modulo operations are applied to all cell indices in $\mathcal{K}$.

Appropriate strategies are necessary for advanced schemes. From previous investigations, system conditions of usage of antennas, CSI and complexity are shown in Table IV, V, VI. There three factors need a balance in the advanced design. In the proposed five approaches, the first approach is a proper basis. It applies cascaded precoders on the BS side. It is proved to be compatible to practical cellular systems to eliminate ICI. While conventionally the cascaded precoders are randomly chosen as in [14], it could be further explored in advanced schemes. Besides, the roles of BSs and MSs need a balance. Usually BSs

have more capability and resources, for example, CSI exchange is more practical via BS backhaul mechanism than via MS conferencing mechanism. However in the broadcast channels to MSs the scheme becomes cumbersome if too many MSs are activated. In summary, the system needs to find a tradeoff with all the above concerns.

B. Advanced Approach for Model 2

Model 2 is discussed here. The approach is similar to the design of [14] with cascaded precoders on the BS side. However, the alignment of ICI could be implemented through different novel options. The advanced process are illustrated as following:

Step 1: Choose an auxiliary intermediate precoder matrix $\mathbf{\Phi}_k \in \mathbb{C}^{N_t \times (M \cdot d)}$ at k-th BS (transmitter), and a second precoder $\tilde{\mathbf{V}}_{k:m} \in \mathbb{C}^{(M \cdot d) \times d}$ preceding the first chosen precoder. Then the actual precoder $\mathbf{V}_{k:m}$ is composed of:

$$\mathbf{V}_{k:m} = \mathbf{\Phi}_k \tilde{\mathbf{V}}_{k:m} \quad m \in \mathcal{M}, k \in \mathcal{K} \tag{62}$$

(Notice the index refers to all equal nodes)

Step 2: When the first precoder $\mathbf{\Phi}_j$ is randomly picked, to enable zero-forcing the ICI from the two adjacent cells, all M users in k-th cell should determine $\mathbf{U}_{k:m}$ to satisfy the following conditions (index changed)

$$\mathbf{U}_{k:m}^{\dagger}[\ \mathbf{H}_{k-1}^{k:m}\mathbf{\Phi}_{k-1}\ \mathbf{H}_{k+1}^{k:m}\mathbf{\Phi}_{k+1}\ ] = \mathbf{0} \quad m \in \mathcal{M} \tag{63}$$

In previous basic schemes, to be feasible to find $\mathbf{U}_{k:m}$, the dimensions should satisfy $N_r \geq 2Md + d$. This requirement is loosened compared with model 1 because the connectivity of the network is lowered. However, even based on the same model of model 2, the antennas could be also further saved with a novel strategy, i.e. as long as the following new condition is satisfied:

$$\mathrm{span}[\mathbf{H}_{k-1}^{k:m}\mathbf{\Phi}_{k-1}] = \mathrm{span}[\mathbf{H}_{k+1}^{k:m}\mathbf{\Phi}_{k+1}] \quad m \in \mathcal{M} \tag{64}$$

When the new condition holds, it is only required that the dimensions satisfy $N_r \geq Md + d$, so that antennas could be saved. Observe equation (64) and important features are concluded in the following remark:

Remark 16: The purpose and essence of condition (64) is to implement an extra alignment in advance on the BS side in addition to the following alignment on the MS side. This alignment is between ICI and ICI from different cells. In principle, this extra condition is natural and reasonable, because $\mathbf{\Phi}_k$ is randomly selected in the conventional scheme as in [14] while in fact the potential could be exploited by selecting appropriate values.

Observe the structure of the condition (64) in the whole cyclic network, it is easy to decompose it into two groups of equations:

$$\begin{aligned}
&\mathrm{span}[\mathbf{H}_i^{i+1:m}\mathbf{\Phi}_i] = \mathrm{span}[\mathbf{H}_{i+2}^{i+1:m}\mathbf{\Phi}_{i+2}] \\
&\qquad i \in \mathcal{K}^{ev} \triangleq \begin{cases} \{2,4,6,\ldots,K\} & K \text{ is even} \\ \{2,4,6,\ldots,K-1\} & K \text{ is odd} \end{cases} \\
&\mathrm{span}[\mathbf{H}_j^{j+1:m}\mathbf{\Phi}_j] = \mathrm{span}[\mathbf{H}_{j+2}^{j+1:m}\mathbf{\Phi}_{j+2}] \\
&\qquad j \in \mathcal{K}^{od} \triangleq \begin{cases} \{1,3,5,\ldots,K-1\} & K \text{ is even} \\ \{1,3,5,\ldots,K\} & K \text{ is odd} \end{cases}
\end{aligned} \tag{65}$$

It means all the conditions in the cells of even numbers are connected and so are the the cells of odd numbers. Since the indices in equation (65) are actually operated in a cyclic mode, e.g. $K \equiv 0$, to explicitly specify the boundary connections between cells at the end of the network, the following equations are highlighted:

$$\begin{aligned}
&\text{For } i \in \mathcal{K}^{ev}, \\
&\quad \begin{cases} \mathrm{span}[\mathbf{H}_K^{1:m}\mathbf{\Phi}_K] = \mathrm{span}[\mathbf{H}_2^{1:m}\mathbf{\Phi}_2] & K \text{ is even} \\ \mathrm{span}[\mathbf{H}_{K-1}^{K:m}\mathbf{\Phi}_{K-1}] = \mathrm{span}[\mathbf{H}_1^{K:m}\mathbf{\Phi}_1] & K \text{ is odd} \end{cases} \\
&\text{For } j \in \mathcal{K}^{od}, \\
&\quad \begin{cases} \mathrm{span}[\mathbf{H}_{K-1}^{K:m}\mathbf{\Phi}_{K-1}] = \mathrm{span}[\mathbf{H}_1^{K:m}\mathbf{\Phi}_1] & K \text{ is even} \\ \mathrm{span}[\mathbf{H}_K^{1:m}\mathbf{\Phi}_K] = \mathrm{span}[\mathbf{H}_2^{1:m}\mathbf{\Phi}_2] & K \text{ is odd} \end{cases}
\end{aligned} \tag{66}$$

In order to satisfy conditions (65) and (66), in the following discussion, five options of designs are proposed and the system conditions are analyzed respectively. For step 2, the five options are marked as: 2a, 2b, 2c, 2d, 2e. Correspondingly, for the subsequent step 3, the five options are marked as: 3a, 3b, 3c, 3d, 3e. For convenience, the following steps are presented in pairs, e.g. 2a combined with 3a.

1) Step 2a,3a: Step 2a: A naive and direct implementation of condition (64) is as following:

$$\mathbf{H}_{k-1}^{k:m}\mathbf{\Phi}_{k-1} = \mathbf{H}_{k+1}^{k:m}\mathbf{\Phi}_{k+1} \quad m \in \mathcal{M} \tag{67}$$

To simplify the discussion, just assume K is even here. So that correspondingly, the conditions of (65) and (66) are implemented as the following equations of $\mathbf{\Phi}_k$:

$$\begin{bmatrix} \vdots & \vdots & & & \\ \mathbf{H}_2^{3:m} & -\mathbf{H}_4^{3:m} & & & \\ \vdots & \vdots & & & \\ & \vdots & \vdots & & \\ & \mathbf{H}_4^{5:m} & -\mathbf{H}_6^{5:m} & & \\ & \vdots & \vdots & & \\ & & & \ddots & \\ \vdots & & & & \vdots \\ -\mathbf{H}_2^{1:m} & & & & \mathbf{H}_K^{1:m} \\ \vdots & & & & \vdots \end{bmatrix} \begin{bmatrix} \mathbf{\Phi}_2 \\ \mathbf{\Phi}_4 \\ \vdots \\ \mathbf{\Phi}_K \end{bmatrix} = \mathbf{0}$$

$$\begin{bmatrix} \vdots & \vdots & & & \\ \mathbf{H}_1^{2:m} & -\mathbf{H}_3^{2:m} & & & \\ \vdots & \vdots & & & \\ & \vdots & \vdots & & \\ & \mathbf{H}_3^{4:m} & -\mathbf{H}_5^{4:m} & & \\ & \vdots & \vdots & & \\ & & & \ddots & \\ \vdots & & & & \vdots \\ -\mathbf{H}_1^{K:m} & & & & \mathbf{H}_{K-1}^{K:m} \\ \vdots & & & & \vdots \end{bmatrix} \begin{bmatrix} \mathbf{\Phi}_1 \\ \mathbf{\Phi}_3 \\ \vdots \\ \mathbf{\Phi}_{K-1} \end{bmatrix} = \mathbf{0} \tag{68}$$

To be feasible to obtain $\mathbf{\Phi}_k$, the dimensions should satisfy $N_t K/2 \geq MN_r K/2 + Md$, i.e. $N_t \geq MN_r + 2Md/K$. When $K \gg M$, it becomes $N_t \geq MN_r$.

Step 3a: Now observe each $\mathbf{\Phi}_k$ again, notice there are $2M$ zero-forcing conditions to satisfy just as the same as in previous section in (26). Normally it is feasible to find $\mathbf{\Phi}_k$ only when $N_t \geq 2Md + Md$. However, if considering (63) already guarantees the condition, it is only required that $N_t \geq Md$ in this process. If further considering (68), as just mentioned, it is required $N_t \geq MN_r$. Notice the mentioned condition $N_r \geq Md + d$. So in summary, when $M \geq 2$, there is no *implicit* alignment on the MS side; only when $M = 1$, there is *implicit* alignment on the MS side.

2) Step 2b,3b:

Step 2b: Notice the above step of (68) has a severe drawback. It needs global CSI and mass calculations which are not reasonable for practical systems. To overcome this drawback, the following process is proposed to implement alignment in a successive manner. According to the condition (65), every $\mathbf{\Phi}_k$ is obtained one by one.

First, two arbitrary cells are set as the initial cells, say $i = 2$, $j = 1$ for the cells of even numbers and odd numbers respectively. Choose random intermediate precoders $\mathbf{\Phi}_i$ and $\mathbf{\Phi}_j$ for both of them. Second, determine receive filters $\mathbf{U}_{i+1:m}$ and $\mathbf{U}_{j+1:m}$ to satisfy the conditions (63), i.e. $\mathbf{U}_{i+1:m}^{\dagger}\mathbf{H}_i^{i+1:m}\mathbf{\Phi}_i = \mathbf{0}$, $\mathbf{U}_{j+1:m}^{\dagger}\mathbf{H}_j^{j+1:m}\mathbf{\Phi}_j = \mathbf{0}$. It's only required that $N_r \geq Md + d$ because the alignment condition (67) guarantees zero-forcing by setting $\mathbf{\Phi}_{i+2}$ and $\mathbf{\Phi}_{j+2}$ in the following cells. Third, according to

(67), $\mathbf{\Phi}_{i+2}$ and $\mathbf{\Phi}_{j+2}$ could be obtained by (pseudo) inverse operations:

$$\begin{aligned}\mathbf{\Phi}_{i+2} &= \left[\begin{Bmatrix}\vdots\\ \mathbf{H}_{i+2}^{i+1:m}\\ \vdots\end{Bmatrix} m\in\mathcal{M}\right]^{-1}\left[\begin{Bmatrix}\vdots\\ \mathbf{H}_{i}^{i+1:m}\\ \vdots\end{Bmatrix} m\in\mathcal{M}\right]\mathbf{\Phi}_i\\ \mathbf{\Phi}_{j+2} &= \left[\begin{Bmatrix}\vdots\\ \mathbf{H}_{j+2}^{j+1:m}\\ \vdots\end{Bmatrix} m\in\mathcal{M}\right]^{-1}\left[\begin{Bmatrix}\vdots\\ \mathbf{H}_{j}^{j+1:m}\\ \vdots\end{Bmatrix} m\in\mathcal{M}\right]\mathbf{\Phi}_j\end{aligned} \tag{69}$$

To be feasible to obtain $\mathbf{\Phi}_{i+2}$ and $\mathbf{\Phi}_{j+2}$ by inverse operations, the dimensions should satisfy $N_t \geq MN_r$. Finally, after completing the whole procedure for all cells, all the other intermediate precoders $\mathbf{\Phi}_{i+4}$, $\mathbf{\Phi}_{j+4}$, $\cdots$, $\mathbf{\Phi}_K$, $\mathbf{\Phi}_1$, $\cdots$, $\mathbf{\Phi}_{i-2}$, $\mathbf{\Phi}_{j-2}$ are obtained. However, notice that the boundary condition (66) is not satisfied. This issue could be ignored considering two reasons. The network may be not circular. The loss of DoF is relatively small to be neglected when K is large.

Step 3b: Now observe each $\mathbf{\Phi}_k$ again, notice there are $2M$ zero-forcing conditions to satisfy just as the same as in previous section in (26). Normally it is feasible to find $\mathbf{\Phi}_k$ only when $N_t \geq 2Md + Md$. However, if further considering (69), as just mentioned, it is required $N_t \geq MN_r$. The requirement is the same as the above step 3a.

3) Step 2c,3c:

Step 2c: Notice the step of (69) has a drawback. It needs a large number of antennas, i.e. N_t is large. To overcome this drawback, the following process is proposed. Compared with Step 2b, $\mathbf{\Phi}_k$ is also obtained in a successive manner, but it utilizes another operation and involves the MS side as well.

First, two arbitrary cells are set as initial cells, say $i = 2$, $j = 1$ for the cells of even numbers and odd numbers respectively. Choose random intermediate precoders $\mathbf{\Phi}_i$ and $\mathbf{\Phi}_j$. Second, determine receive filters $\mathbf{U}_{i+1:m}$ and $\mathbf{U}_{j+1:m}$ to satisfy half of the condition (63), i.e. $\mathbf{U}_{i+1:m}^{\dagger}\mathbf{H}_i^{i+1:m}\mathbf{\Phi}_i = \mathbf{0}$, $\mathbf{U}_{j+1:m}^{\dagger}\mathbf{H}_j^{j+1:m}\mathbf{\Phi}_j = \mathbf{0}$. It's only required that $N_r \geq Md + d$ as mentioned. Third, according to the other half of the condition (63), $\mathbf{\Phi}_{i+2}$ and $\mathbf{\Phi}_{j+2}$ could be obtained by alternative null space operations:

$$\begin{aligned}\mathbf{\Phi}_{i+2} &= \mathrm{null}(\left[\begin{Bmatrix}\vdots\\ \mathbf{U}_{i+1:m}^{\dagger}\mathbf{H}_{i+2}^{i+1:m}\\ \vdots\end{Bmatrix} m\in\mathcal{M}\right])\\ \mathbf{\Phi}_{j+2} &= \mathrm{null}(\left[\begin{Bmatrix}\vdots\\ \mathbf{U}_{j+1:m}^{\dagger}\mathbf{H}_{j+2}^{j+1:m}\\ \vdots\end{Bmatrix} m\in\mathcal{M}\right])\end{aligned} \tag{70}$$

Remark 17: To be feasible to obtain $\mathbf{\Phi}_{i+2}$ and $\mathbf{\Phi}_{j+2}$ by null space operations, the dimensions should satisfy $N_t \geq Md+Md$. So that BS antennas only require $N_t \geq 2Md$, which is enormously reduced compared with Step 2a and Step 2b. Thanks to the successive implicit alignment involving precoders, receive filters in a cooperative way. This successive manner obtains BS precoder $\mathbf{\Phi}_k$ and MS receive filter $\mathbf{U}_{k:m}$ alternatively like 'bounces' between two sides, saving both huge antenna usage and global CSI exchange resulting in a chain connecting all the coders.

Finally, after completing the whole procedure for all cells, all the other intermediate precoders $\mathbf{\Phi}_{i+4}$, $\mathbf{\Phi}_{j+4}$, $\cdots$, $\mathbf{\Phi}_K$, $\mathbf{\Phi}_1$, $\cdots$, $\mathbf{\Phi}_{i-2}$, $\mathbf{\Phi}_{j-2}$ are obtained. As mentioned in Step 2b, the boundary condition (66) could be ignored.

Step 3c: Now observe each $\mathbf{\Phi}_k$ again, notice there are $2M$ zero-forcing conditions to satisfy just as in previous section in (26). Normally, it is required $N_t \geq 2Md+Md$. However, further consider the condition (63) to obtain $\mathbf{U}_{k:m}$ and the operation (70) to obtain $\mathbf{\Phi}_k$, the alignment is successfully implemented on both BS side and MS side by zero-forcing:

$$\begin{aligned}&(\mathbf{U}_{k-1:m}^{\dagger}\mathbf{H}_k^{k-1:m})\mathbf{\Phi}_k = (\mathbf{U}_{k+1:m}^{\dagger}\mathbf{H}_k^{k+1:m})\mathbf{\Phi}_k \quad m\in\mathcal{M}\\ &\mathbf{U}_{k:m}^{\dagger}(\mathbf{H}_{k-1}^{k:m}\mathbf{\Phi}_{k-1}) = \mathbf{U}_{k:m}^{\dagger}(\mathbf{H}_{k+1}^{k:m}\mathbf{\Phi}_{k+1}) \quad m\in\mathcal{M}\end{aligned} \tag{71}$$

In summary, for BS antennas, it is only required $N_t \geq 2Md$ instead of previous requirement $N_t \geq 3Md$; for MS antennas, it is only required $N_r \geq Md+d$ instead of previous requirement $N_r \geq 2Md+d$. The antenna usage is greatly saved to obtain more DoF.

4) Step 2d,3d:

Step 2d: Since Step 2b needs a large number of antennas and Step 2c needs successive CSI exchange between BS side and MS side as well as a lot of computations, the following process is proposed to further reduce the usage of antennas and to focus on the BS side. It applies a robust measure to implement the alignment in a flexible and compatible way. The new process deals with the condition of (65) by utilizing a metric called *chordal distance*.

For each BS, the precoder $\mathbf{\Phi}_k$ is set to be only selected from a finite predefined set named as $\mathfrak{B}_k$. Then the whole procedure is similar to Step 2b. First, two initial cells 2 and 1 are set for even numbers and odd numbers respectively. Choose $\mathbf{\Phi}_i$ and $\mathbf{\Phi}_j$ for them. Second, determine receive filters $\mathbf{U}_{i+1:m}$ and $\mathbf{U}_{j+1:m}$. Third, obtain $\mathbf{\Phi}_{i+2}$ and $\mathbf{\Phi}_{j+2}$. Instead of the inverse operations in (69), the new operations are approximations by selecting the most aligned ICI with the metric of chordal distance:

$$\begin{aligned}\mathbf{\Phi}_{i+2} &= \arg \min_{\mathbf{\Phi}_{i+2}\in\mathfrak{B}_{i+2}} \sum_{m=1}^{M} D_c^2(\mathbf{H}_i^{i+1:m}\mathbf{\Phi}_i, \mathbf{H}_{i+2}^{i+1:m}\mathbf{\Phi}_{i+2}) \\ \mathbf{\Phi}_{j+2} &= \arg \min_{\mathbf{\Phi}_{j+2}\in\mathfrak{B}_{j+2}} \sum_{m=1}^{M} D_c^2(\mathbf{H}_j^{j+1:m}\mathbf{\Phi}_j, \mathbf{H}_{j+2}^{j+1:m}\mathbf{\Phi}_{j+2})\end{aligned} \tag{72}$$

In equation (72), $D_c(\cdot,\cdot)$ denotes the chordal distance used as the metric of alignment as in [26], [37]. Mathematically, the chordal distance between two $N_r \times Md$ matrices $\mathbf{P}$ and $\mathbf{Q}$ is defined as:

$$\begin{aligned}&D_c^2(\mathbf{P},\mathbf{Q}) = D_c^2(\mathbb{O}(\mathbf{P}),\mathbb{O}(\mathbf{Q})) \\ &= \frac{1}{2}\|\mathbb{O}(\mathbf{P})\mathbb{O}(\mathbf{P})^\dagger - \mathbb{O}(\mathbf{Q})\mathbb{O}(\mathbf{Q})^\dagger\|_F \\ &= Md - \mathrm{Trace}(\mathbb{O}(\mathbf{P})^\dagger\mathbb{O}(\mathbf{Q})\mathbb{O}(\mathbf{Q})^\dagger\mathbb{O}(\mathbf{P}))\end{aligned} \tag{73}$$

where $\mathbb{O}(\mathbf{P})$ and $\mathbb{O}(\mathbf{Q})$ are orthonormal bases of $\mathbf{P}$ and $\mathbf{Q}$ respectively.

To be feasible to obtain $\mathbf{\Phi}_{i+2}$ and $\mathbf{\Phi}_{j+2}$ by selections of chordal distances, it is only required the dimensions should satisfy $N_t \geq Md$ rather than $N_t \geq MN_r$ in Step 2b or $N_t \geq 2Md$ in Step 2c. In principle, the condition (67) $\mathbf{H}_{k-1}^{k:m}\mathbf{\Phi}_{k-1} = \mathbf{H}_{k+1}^{k:m}\mathbf{\Phi}_{k+1}$ is too tight for Step 2b, and the condition (72) actually relaxes it to $\mathrm{span}[\mathbf{H}_{k-1}^{k:m}\mathbf{\Phi}_{k-1}] = \mathrm{span}[\mathbf{H}_{k+1}^{k:m}\mathbf{\Phi}_{k+1}]$. However, when $N_t < 2Md$, the alignment could not be perfect and there is still residue interference for sure which degrades the performance severely. Anyway, it provides an accessible way to approach alignment under the situation with few antennas.

Step 3d: Now observe each $\mathbf{\Phi}_k$ again, notice there are $2M$ zero-forcing conditions to satisfy just as the same as in previous section in (26). The conditions are partially satisfied by (72). Other requirements are the same as Step 3b and 3c.

In summary, Step 2d applies the precoder selection method. It has a few advantages. Antenna requirement is significantly lowered; CSI is reduced by only exchanging precoder indices; computational complexity to satisfy condition (65) is saved a lot; the system complicacy is simplified. It also has a few disadvantages. The residue inter-cell interference (ICI) definitely causes rate and DoF loss, although the loss is not severe if considering large path loss of ICI. While conventional opportunistic selection method only selects one best MS in each cell with other MSs inactive [26], [38]. When there are enough number of MSs, the performance of the selected MS is is always good because of the selection diversity. In this work the process enable all the MSs in all cells to be active. The selection is proceeded on the precoder matrices at BSs to approach alignment. Actually it takes a tradeoff between the usage of antennas and the system performance. Compared with pure analytical designs, the system conditions are simplified. Although it is unlikely to be optimal, the effort of this process is to ensure acceptable performance.

5) Step 2e,3e:

Step 2e: Since Step 2c applies a different successive approach between BS side and MS side and still uses a lot of antennas, the following process is proposed to improve them by applying a robust measure to implement the alignment of condition (63) in a flexible and compatible way. The new process utilizes a metric called *interference leakage*.

The whole procedure is similar to Step 2c. First, two initial cells 2 and 1 are set for even numbers and odd numbers respectively. Choose $\mathbf{\Phi}_i$ and $\mathbf{\Phi}_j$ for them. Second, determine receive filters $\mathbf{U}_{i+1:m}$ and $\mathbf{U}_{j+1:m}$. Third, obtain $\mathbf{\Phi}_{i+2}$ and $\mathbf{\Phi}_{j+2}$. Instead of the null space operations in (70), the new operations are approximations by selecting the minimized ICI with the metric of interference leakage:

$$\begin{aligned}\mathbf{\Phi}_{i+2} &= \arg \min_{\mathbf{\Phi}_{i+2}^\dagger\mathbf{\Phi}_{i+2}=\mathbf{I}_{Md}} \sum_{m=1}^{M} L_{IF}(\mathbf{U}_{i+1:m}, \mathbf{H}_{i+2}^{i+1:m}\mathbf{\Phi}_{i+2}) \\ \mathbf{\Phi}_{j+2} &= \arg \min_{\mathbf{\Phi}_{j+2}^\dagger\mathbf{\Phi}_{j+2}=\mathbf{I}_{Md}} \sum_{m=1}^{M} L_{IF}(\mathbf{U}_{j+1:m}, \mathbf{H}_{j+2}^{j+1:m}\mathbf{\Phi}_{j+2})\end{aligned} \tag{74}$$

In equation (74), $L_{IF}(\cdot,\cdot)$ denotes interference leakage as the metric of alignment as in [26], [39].Mathematically, interference leakage on the receive matrix $\mathbf{P}$ from the interference source matrix $\mathbf{Q}$ is defined as:

$$L_{IF}(\mathbf{P},\mathbf{Q}) = \mathrm{Trace}((\mathbf{P}^{\dagger}\mathbf{Q})(\mathbf{P}^{\dagger}\mathbf{Q})^{\dagger}) \tag{75}$$

While the solution to the minimization problem (74) is given by:

$$\begin{aligned}\mathbf{\Phi}_{i+2} &= \nu_{Md}\Big\{\sum_{m=1}^{M}(\mathbf{H}_{i+2}^{i+1:m})^{\dagger}\mathbf{U}_{i+1:m}\mathbf{U}_{i+1:m}^{\dagger}\mathbf{H}_{i+2}^{i+1:m}\Big\}\\ \mathbf{\Phi}_{j+2} &= \nu_{Md}\Big\{\sum_{m=1}^{M}(\mathbf{H}_{j+2}^{j+1:m})^{\dagger}\mathbf{U}_{j+1:m}\mathbf{U}_{j+1:m}^{\dagger}\mathbf{H}_{j+2}^{j+1:m}\Big\}\end{aligned} \tag{76}$$

where $\nu_{Md}\{\cdot\}$ is composed of Md eigenvectors corresponding to the smallest Md eigenvalues of the matrix.

To be feasible to obtain $\mathbf{\Phi}_{i+2}$ and $\mathbf{\Phi}_{j+2}$ by leakage minimization, it is only required the dimensions should satisfy $N_t \geq Md$ rather than $N_t \geq 2Md$ in Step 2c. Because the condition (70) actually guarantees the interference leakage is absolutely zero, which is a tight constraint. However, the robust measure allows an imperfect alignment and residue interference leakage as well as corresponding DoF loss in the practice.

Step 3e: Now observe each $\mathbf{\Phi}_k$ again, the zero-forcing conditions in (26) are partially satisfied. Other requirements are the same as Step 3c.

In summary, this robust measure of interference leakage minimization is adaptable to a wider range of antenna configurations. The performance of rate and DoF are controllable and amendable regarding the usage of antennas. When there are enough antennas, perfect alignment could be achieved. When there are less antennas, partial alignment with residue interference is obtained.

Step 4: Following Step 2 and Step 3 (with options: a,b,c,d,e respectively), then each k-th BS knows its equivalent downlink channel $\mathbf{U}_{k:m}\mathbf{H}_k^{k:m}\mathbf{\Phi}_k$ from each intra-cell MS. It forms zero-forcing transmit beams which could eliminate IUI between the MSs, while it does not need to know the actual interfering beams. The second precoder matrix is obtained by the following inverse operation:

$$\Big[\tilde{\mathbf{V}}_{k:1}\ \tilde{\mathbf{V}}_{k:2}\ \cdots\ \tilde{\mathbf{V}}_{k:M}\Big] = \begin{bmatrix}\mathbf{U}_{k:1}^{\dagger}\mathbf{H}_k^{k:1}\mathbf{\Phi}_k\\ \mathbf{U}_{k:2}^{\dagger}\mathbf{H}_k^{k:2}\mathbf{\Phi}_k\\ \vdots\\ \mathbf{U}_{k:M}^{\dagger}\mathbf{H}_k^{k:M}\mathbf{\Phi}_k\end{bmatrix}^{-1} \tag{77}$$

C. Advanced Approach for Model 3

Model 3 is discussed here. In this Wyner-type network, there is only one adjacent link for each cell. So that a new approach is specifically proposed to fit this model. This advanced process takes four steps as following:

Step 1: Choose a random receive filter $\mathbf{U}_{k:m^{\star}}$ for each $m^{\star}$-th MS among all $M^{\star}$ cell-interior MSs in the k-th cell. Also choose a random receive filter $\mathbf{U}_{k:m^{\circ}}$ for each m°-th MS among all M° cell-edge MSs in the k-th cell. To be feasible to obtain $\mathbf{U}_{k:m^{\star}}$ and $\mathbf{U}_{k:m^{\circ}}$ for available transmissions, it is only required the dimensions should satisfy $N_r^{\star} \geq d$ and $N_r^{\circ} \geq d$.

Step 2: Because of the special structure of model 3, it is not necessary to apply intermediate precoder $\mathbf{\Phi}_k$ at k-th BS as in [14]. So that the precoders need to satisfy all the zero-forcing conditions directly. Each $\mathbf{V}_{k:m}$ for the m-th user in the k-the cell has $(M^{\circ}+M-1)$ zero-forcing conditions as following:

$$\begin{bmatrix}\vdots\\ \mathbf{U}_{k-1:m^{\circ}}^{\dagger}\mathbf{H}_k^{k-1:m^{\circ}}\\ \vdots\\ \vdots\\ \mathbf{U}_{k:n}^{\dagger}\mathbf{H}_k^{k:n}\\ \vdots\end{bmatrix}\begin{matrix}\left.\begin{matrix}\\ \\ \\ \end{matrix}\right\} m^{\circ}\in\mathcal{M}^{\circ}\\ \left.\begin{matrix}\\ \\ \end{matrix}\right\} n\in\mathcal{M}\backslash\{m\}\end{matrix}\mathbf{V}_{k:m} = \mathbf{0} \tag{78}$$

Option	Minimum BS Antenna.	Minimum MS Antenna
a	$MN_r + 2Md/K$	$Md + d$
b	MN_r	$Md + d$
c	$2Md$	$Md + d$
d	Md	$Md + d$
e	Md	$Md + d$

TABLE X
MINIMUM ANTENNA USAGE FOR BSS AND MSS IN THE ADVANCED APPROACH FOR MODEL 2

The condition (78) represents that the ICI from the k-th BS to cell-edge MSs in the $(k-1)$-th cell is zero and the IUI between the m-th MS and other MSs in the k-th cell is zero.

Step 3: Then each k-th BS knows its equivalent downlink channel $\mathbf{U}_{k-1:m^\circ}\mathbf{H}_k^{k-1:m^\circ}$ from MSs in the $(k-1)$-th cell and $\mathbf{U}_{k:m}\mathbf{H}_k^{k:m}$ from its own intra-cell MSs. It forms zero-forcing transmit beams to eliminate both ICI and IUI together as following:

$$[\mathbf{V}_{k:1}\ \mathbf{V}_{k:2}\ \cdots\ \mathbf{V}_{k:M}] = \text{The last } Md \text{ columns of} \left[\begin{array}{c} \vdots \\ \mathbf{U}_{k-1:m^\circ}^\dagger \mathbf{H}_k^{k-1:m^\circ} \\ \vdots \end{array}\right\} m^\circ \in \mathcal{M}^\circ \left.\begin{array}{c} \\ \\ \\ \\ \vdots \\ \mathbf{U}_{k:m}^\dagger \mathbf{H}_k^{k:m} \\ \vdots \end{array}\right\} m \in \mathcal{M} \Bigg]^{-1} \tag{79}$$

Check condition (78) and condition (79). Both of them require the dimensions should satisfy $N_t \geq M^\circ d + Md$.

Step 4: Observe the receive filters $\mathbf{U}_{k:m^\circ}$ and $\mathbf{U}_{k:m^\star}$ again, notice there are $(2M-1)$ and $(M-1)$ zero-forcing conditions to satisfy respectively.

$$\begin{aligned} \mathbf{U}_{k:m^\circ}^\dagger [\underbrace{\cdots \mathbf{H}_k^{k:m^\circ}\mathbf{V}_{k:n}\cdots}_{n\in\mathcal{M}\setminus\{m^\circ\}}\ \underbrace{\cdots \mathbf{H}_{k+1}^{k:m^\circ}\mathbf{V}_{k+1:m}\cdots}_{m\in\mathcal{M}}] &= \mathbf{0} \\ \mathbf{U}_{k:m^\star}^\dagger [\underbrace{\cdots \mathbf{H}_k^{k:m^\star}\mathbf{V}_{k:n}\cdots}_{n\in\mathcal{M}\setminus\{m^\star\}}] &= \mathbf{0} \end{aligned} \tag{80}$$

Remark 18: Check the condition (80). Normally, it is feasible to find $\mathbf{U}_{k:m^\circ}$ and $\mathbf{U}_{k:m^\star}$ only when the dimensions satisfy $N_r^\circ \geq (M-1)d + Md + d$ and $N_r^\star \geq (M-1)d + d$ respectively. However, since (78) and (79) already guarantee this condition, it is only required that $N_r^\circ \geq d$ and $N_r^\star \geq d$ in this specific design process. So this process naturally contains an *implicit* and *inherent* alignment.

In summary, the four steps determine receive filters and precoders in one time because of the connectivity is loose in this network. Alignment is implemented on the receiver side.

D. Comparison of System Conditions

Similar to the basic designs and analyses for model 1, model 2, and model 3, system conditions are listed and compared here for the advanced approaches for model 2 and model 3. Three aspects are investigated including the usage of antennas, CSI exchange, and computational complexity.

1) DoF and Antenna Range: For the advanced approach of model 2, there are five options of Step 2 and Step 3. All the antenna configurations for these options are listed in Table X respectively. The notations 'a','b','c','d','e' denote them in sequence. Compared with the antenna configurations in Table IV for the basic design of model 2, the antenna usage is greatly reduced.

For the advanced approach of model 3, the antenna configuration is listed in Table XI, which is denoted as 'F' for consistency. Compared with the antenna configuration in Table VII for the basic design of model 3, the antenna usage is greatly reduced.

In summary, the number of antennas plays a key role to implement alignment and the antennas could have different balance between BS side and MS side to achieve alignment. The aim of this work is exploit interference alignment with limited provision of antennas. Among the five options of model 2, options 'c', 'd', and 'e' use less antennas for the BS side. Notice

Approach	Minimum BS Antenna.	Minimum MS Antenna $(N_r^\star, N_r^\circ)$
F	$M^\circ d + Md$	(d, d)

TABLE XI
MINIMUM ANTENNA USAGE FOR BSS AND MSS IN THE ADVANCED APPROACH FOR MODEL 3

options 'd' and 'e' apply robust measures so that there are residue interferences due to minimizing the number of antennas. For model 3, BS side uses extra antennas to deal with interference while MS side uses the minimum number of antennas.

2) CSI Overhead: For the advanced approach of model 2, there are five options of Step 2 and Step 3. All the CSI configurations for these options are listed in Table XII. The notations 'a','b','c','d','e' denote them in sequence. Compared with the CSI overhead in Table V for the basic design of model 2, the CSI requirement is lowered much.

Option	required extra CSI at k-th BS (besides: all intra-cell MSs, $\mathbf{U}_{k:m}^\dagger \mathbf{H}_k^{k:m}$, M)		
	Source	Content	Quantity
a	adjacent inter-cell MSs (excl. backhaul)	$\mathbf{H}_k^{k-1:m}, \mathbf{H}_k^{k+1:m}$	M, M
b	adjacent inter-cell MSs preceding-adjacent inter-cell MSs	$\mathbf{H}_{k-2}^{k-1:m}\mathbf{\Phi}_{k-2}$ $\mathbf{H}_k^{k-1:m}$	M, M
c	adjacent inter-cell MSs	$\mathbf{U}_{k-1:m}^\dagger \mathbf{H}_k^{k-1:m}$	M
d	adjacent inter-cell MSs preceding-adjacent inter-cell MSs	$\mathbf{H}_{k-2}^{k-1:m}\mathbf{\Phi}_{k-2}$ $\mathbf{H}_k^{k-1:m}$	M, M
e	adjacent inter-cell MSs	$\mathbf{U}_{k-1:m}^\dagger \mathbf{H}_k^{k-1:m}$	M

Option	required CSI at m-th MS in k-th cell		
	Source	Content	Quantity
a	adjacent inter-cell BS	$\mathbf{H}_{k-1}^{k:m}\mathbf{\Phi}_{k-1}$	1
b	adjacent inter-cell BS	$\mathbf{H}_{k-1}^{k:m}\mathbf{\Phi}_{k-1}$	1
c	adjacent inter-cell BS	$\mathbf{H}_{k-1}^{k:m}\mathbf{\Phi}_{k-1}$	1
d	adjacent inter-cell BS	$\mathbf{H}_{k-1}^{k:m}\mathbf{\Phi}_{k-1}$	1
e	adjacent inter-cell BS	$\mathbf{H}_{k-1}^{k:m}\mathbf{\Phi}_{k-1}$	1

TABLE XII
CSI FOR BSS AND MSS IN THE ADVANCED APPROACH FOR MODEL 2

For the advanced approach of model 3, the CSI configuration is listed in Table XIII, which is denoted as 'F' for consistency. Compared with the CSI overhead in Table VIII for the basic design of model 3, the CSI requirement is lowered much.

Approach	required CSI at k-th BS from Interior and Edge MSs $(m^\star, m^\circ)$		
	Source	Content	Quantity
F	all intra-cell MSs adjacent inter-cell MSs	$(\mathbf{U}_{k:m^\star}^\dagger \mathbf{H}_k^{k:m^\star}, \mathbf{U}_{k:m^\circ}^\dagger \mathbf{H}_k^{k:m^\circ})$ $(/, \mathbf{U}_{k-1:m^\circ}^\dagger \mathbf{H}_k^{k-1:m^\circ})$	$(M^\star, M^\circ)$ $(/, M^\circ)$

Approach	required CSI at m-th MS in k-th cell $(m^\star, m^\circ)$		
	Source	Content	Quantity
F	/	$(/, /)$	/

TABLE XIII
CSI FOR BSS AND MSS IN THE ADVANCED APPROACH FOR MODEL 3

In summary, the proposed interference alignment approaches require all the BS nodes and MS nodes to have certain knowledge of channel state information (CSI). The aim of this work is look for the lowest CSI requirement for the network in different approaches. Among the five options of model 2, options 'c' and 'e' need less CSI for the BS side. For model 3, only BS side needs CSI.

3) Computational Complexity: For the advanced approach of model 2, there are five options of Step 2 and Step 3. All the complexity configurations are listed in Table XIV. The notations 'a','b','c','d','e' denote them in sequence. Compared with the computational complexity in Table VI for the basic design of model 2, the expended complexity is reduced a lot.

For the advanced approach of model 3, all the complexity configurations are listed in Table XV, which is denoted as 'F' for consistency. Compared with the complexity in Table IX for the basic design of model 3, the expended complexity is reduced a lot.

Option	Expended complexity at k-th BS (besides: $\tilde{\mathbf{V}}_{k:m}$, matrix inverse, $Md \times Md$)		
	Target	Operation	Scale
a	$\mathbf{\Phi}_k$	null space	$N_t K/2 \times Md$ (for $K/2$ BSs)
b	$\mathbf{\Phi}_k$	matrix inverse	$N_t \times MN_r$
c	$\mathbf{\Phi}_k$	null space	$N_t \times Md$
d	$\mathbf{\Phi}_k$	chordal distance	$N_r \times Md \times \lvert\mathfrak{B}_k\rvert \times M$
e	$\mathbf{\Phi}_k$	trace	$d \times Md \times \lvert\mathfrak{B}_k\rvert \times M$

Option	Expended complexity at m-th MS in k-th cell		
	Target	Operation	Scale
a	$\mathbf{U}_{k:m}$	null space	$N_r \times d$
b	$\mathbf{U}_{k:m}$	null space	$N_r \times d$
c	$\mathbf{U}_{k:m}$	null space	$N_r \times d$
d	$\mathbf{U}_{k:m}$	null space	$N_r \times d$
e	$\mathbf{U}_{k:m}$	null space	$N_r \times d$

TABLE XIV
COMPLEXITY FOR BSS AND MSS IN THE ADVANCED APPROACH FOR MODEL 2

Approach	Expended complexity at k-th BS		
	Target	Operation	Scale
F	$\mathbf{V}_{k:m}$	matrix inverse	$(M^{\circ}d + Md) \times N_t$

Approach	Expended complexity at m-th MS in k-th cell $(m^{\star}, m^{\circ})$		
	Target	Operation	Scale
F	$(/, /)$	/	/

TABLE XV
COMPLEXITY FOR BSS AND MSS IN THE ADVANCED APPROACH FOR MODEL 3

In summary, all the nodes need to calculate their coding matrices or filters with obtained CSI. The aim of this work is to look for the minimum computational complexities for the network in different approaches. Among the five options for model 2, option 'c' needs a small computational complexity. For model 3, only BS side needs computational complexity.

E. Numerical Results

The previous parts of this work give detailed designs and analyses in various models with different approaches. System conditions and performance are listed and compared. The result indicates that some of them are quite fit to be applicable to current cellular network frameworks. In the following part, numerical results are illustrated to evaluate the rates and DoF performance impacted by key factors. Model 2 is intensively studied and model 3 is also investigated. Advanced approaches are compared with some basic approaches. An main focus is on the usage of antennas and achievable DoF.

All the figures show the total achievable rates as the SNR grows so that DoF is well illustrated. To present it in a intuitive way, the SNR applies a $\log_2$ operation so that DoF is exactly the slope of the corresponding curve. For all the discussion, the network is set to have $K = 6$ cells totally. Each cell has $M = 3$ MSs and each MS has $d = 2$ streams.

1) Model 2 in Different Cases: For model 2, numerical results of five cases are compared as shown in Fig. 4. In the first case, the basic approach 1 is applied as a reference. So that the antennas are set as $N_t = Md = 6$ for each BS and $N_r = 2Md + d = 14$ antennas for each MS. In the second case, option 'b' of the advanced approach is applied. The antennas are set as $N_t = MN_r = 24$ for each BS and $N_r = Md + d = 8$ for each MS. In the third case, option 'c' of the advanced approach is applied. The antennas are set as $N_t = 2Md = 12$ for each BS and $N_r = Md + d = 8$ for each MS. In the fourth case, option 'd' of the advanced approach is applied. The antennas are set as $N_t = Md = 6$ for each BS and $N_r = Md + d = 8$ for each MS. In the fifth case, option 'e' of the advanced approach is applied. The antennas are set as $N_t = Md = 6$ antennas for each BS and $N_r = Md + d = 8$ antennas for each MS.

From Fig. 4, observe that the basic approach and the options 'b', 'c', and 'e' of the advanced approach obtain effective DoF for the network while the option 'd' of the advanced approach has zero DoF. The slope of the basic approach is higher than the advanced approach, because the basic approach applies a perfect alignment for the whole network symmetrically while the advanced approach ignores the DoF loss of the boundary cells in the network as mentioned although the antenna usage is greatly reduced. The option 'd' of the advanced approach causes residue interference due to finite precoder selections so that it is not an absolute alignment in term of DoF.

2) Model 2 with Cascaded Precoders regarding Antenna Number and Codebook Size: Although the DoF is zero for the option 'd' of the advanced approach for model 2 as mentioned above, it is necessary to look into its rate performance since

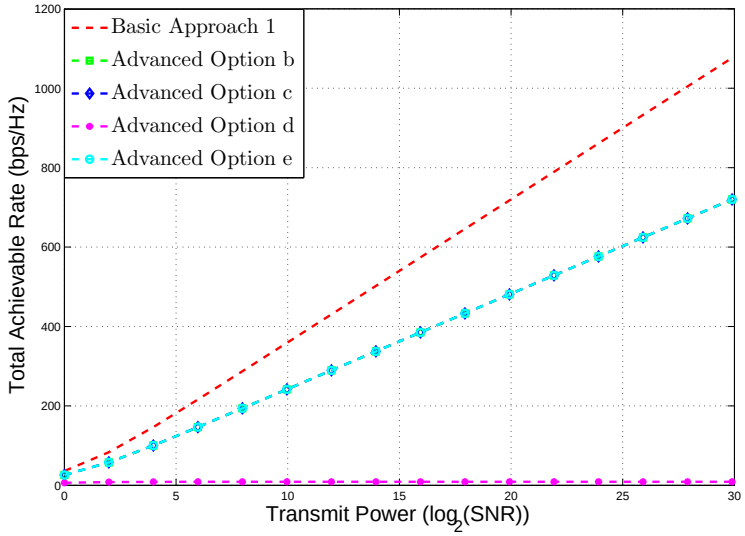

Fig. 4. Rates of Model 2 in Different Cases of Approaches

this options is proposed as a robust measure to obtain performance under the condition of scarce antennas. Intuitively, two factors impact the final performance. One is the number of antennas, the other is the size of codebooks. Numerical results are compared in Fig. 5 and Fig. 6 respectively.

In Fig. 5, option 'd' of the advanced approach is applied and different numbers of BS antennas N_t are compared. The antennas are set as $N_r = Md + d = 8$ for each MS and $N_t = 6, 7, 12, 16, 24$ for each BS. Notice the key values $N_t = Md = 6$, $N_t = 2Md = 12$ and $N_t = MN_r = 24$. Then Fig. 5 shows five curves corresponding to different values of N_t. From Fig. 5, observe that when there are more extra BS antennas, the residue interference is lower. So that the rates increase because the alignment is better.

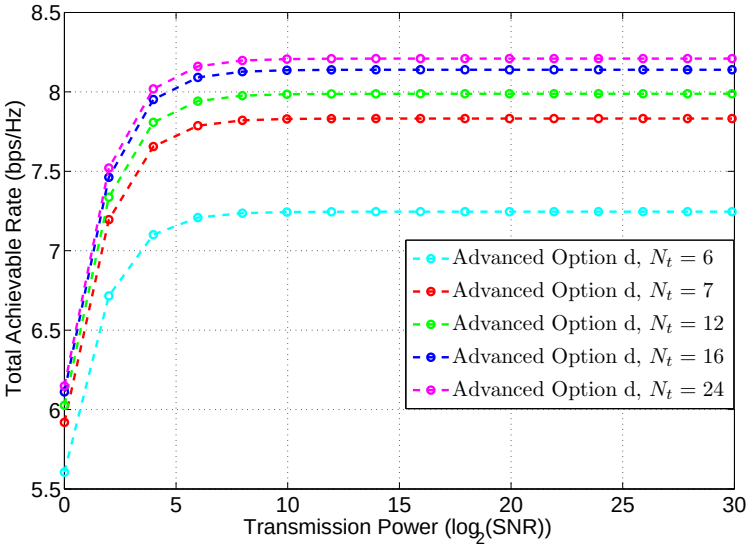

Fig. 5. Rates of Model 2 with Cascaded Precoders regarding Antenna Number

In Fig. 6, option 'd' of the advanced approach is applied and different sizes of the selection set of $|\mathfrak{B}_k|$ are compared. The antennas are set as $N_r = 8$ for each MS and $N_t = 12$ for each BS. The sizes of $|\mathfrak{B}_k|$ are set as 1, 20, and 200. Then Fig. 6 shows three curves corresponding to different sizes of $|\mathfrak{B}_k|$. From 6, observe that when the size of the selection set grows,

the residue interference decreases. So that the rates increase because the alignment is better.

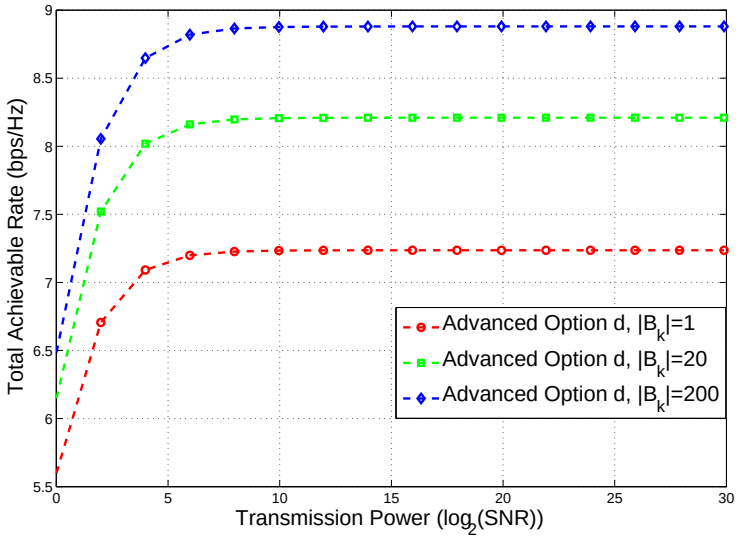

Fig. 6. Rates of Model 2 with Cascaded Precoders regarding Codebook Size

3) Model 2 with Interference Leakage regarding Abundant and Scarce BS antennas: Since option 'd' and option 'e' are two robust measures of alignment for model 2, and the above results show that option 'd' has only zero DoF with precoder selection, the following results investigate option 'e' could obtain appropriate DoF and rates depending on the number of BS antennas. In Fig. 7, different numbers of antennas N_t are compared from $N_t = Md = 6$ to $N_t = Md + Md = 12$. It is set as $N_t = 6, 7, 9, 10, 11$ and 12. Then Fig. 7 show six curves corresponding to different values of N_t. From Fig. 7, observe that when $N_t = 12$ the network obtains full designed DoF and when $N_t = 11$, the network still obtains half designed DoF. When $N_t < 11$, the network has zero DoF due to residue interference.

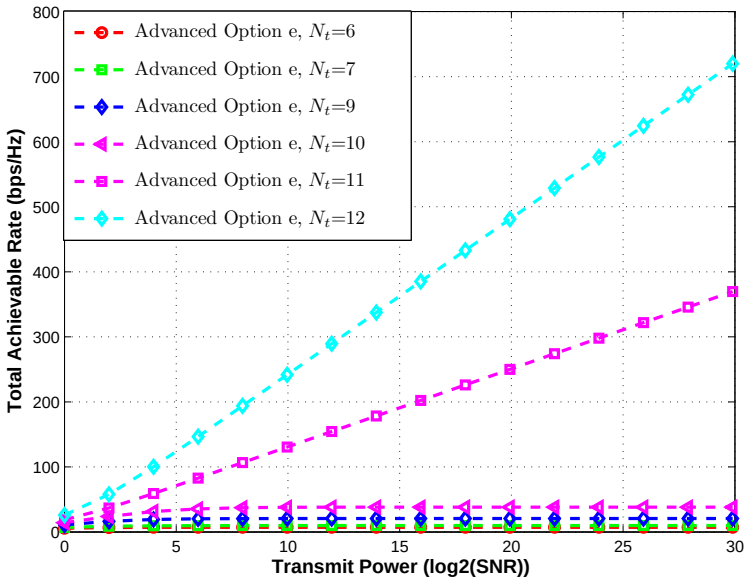

Fig. 7. Rates of Model 2 with Interference Leakage with Abundant and Scarce BS antennas

Fig. 8 shows the four curves of $N_t = 6, 7, 9, 10$ from Fig. 7 separately in a zoomed view. From Fig. 8, observe that when the BS antennas grows, the residue interference decreases. So that the rates increase because the alignment is getting better.

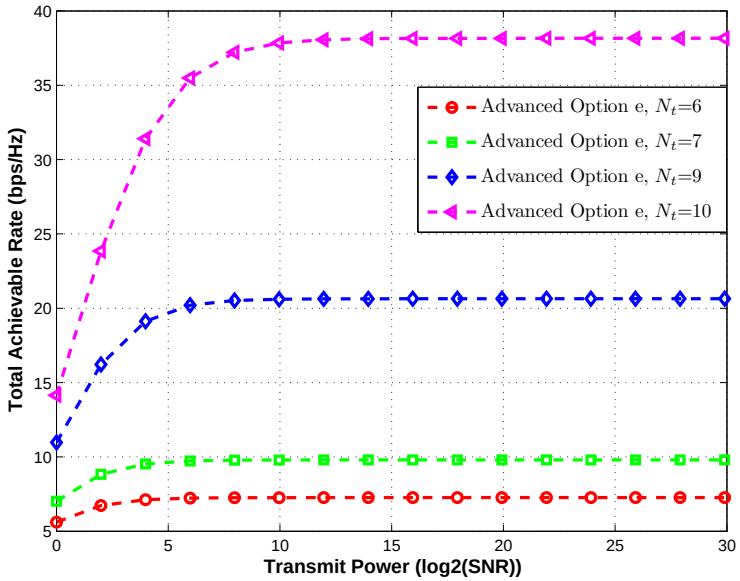

Fig. 8. Rates of Model 2 with Interference Leakage with Scarce BS antennas

4) Model 3 with Basic and Advanced Approaches: For model 3, numerical results of the basic approach and advanced approach are compared as in Fig. 9. The network also has $K = 6$ cells. However, each cell has $M^\star = 3$ cell-interior MSs and $M^\circ = 2$ cell-edge MSs. Each user has $d = 2$ streams. In the first case, the basic approach 1 is applied as a reference, i.e. with cascaded precoders on BS side. The antennas are set as $N_t = Md = 10$ for each BS, $N_r = d = 2$ for each cell-interior MS and $N_r = Md + d = 12$ for each cell-edge MS. In the second case, the advanced approach is applied. The antennas are set as $N_t = M^\circ d + Md = 14$ for each BS, $N_r = d = 2$ for each cell-interior MS and $N_r = d = 2$ for each cell-edge MS. From Fig. 9, observe that both the basic approach and the advanced approach obtain full DoF. Nevertheless, the advanced approach has a lower usage of antennas in the whole.

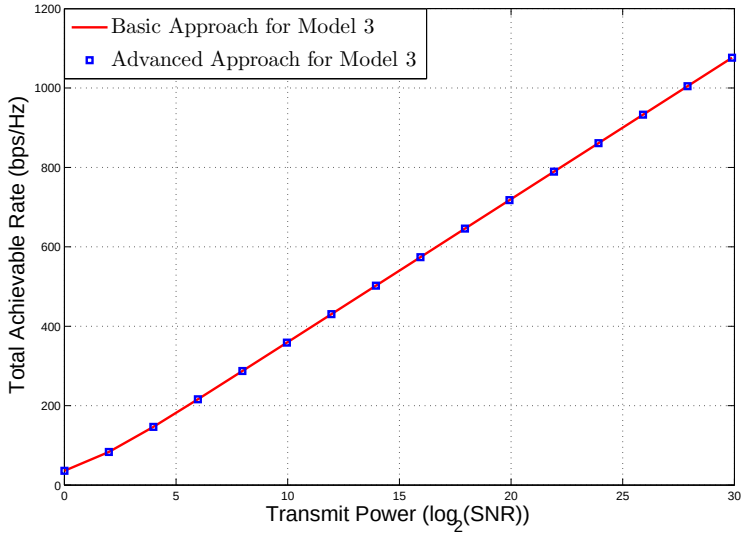

Fig. 9. Rates of Model 3 with Basic and Advanced Approaches

VII. Conclusion

This work generalizes the design and analysis of interference alignment in downlink channels of the multi-cell multi-user network. In such a complicated network, it is necessary to deal with both inter-user interference (IUI) and inter-cell interference (ICI). Conventional alignment schemes for peer-to-peer interference channels (IC) are not available to handle cellular networks. Also conventional alignment schemes for two-cell networks are not robust enough to settle multi-cell networks. Therefore, novel approaches are proposed and compared for typical multi-cell networks. For practical concerns, the Wyner-type networks are particularly investigated. According to the broadcast nature of the cellular networks, the alignment could be implemented from both the BS side and the MS side to achieve a reasonable balance. The alignment process is also in a dynamic manner to form all the coders. System conditions of antennas, CSI, and complexity are compared deliberately. Advanced approaches exploit the network structure to further save the usage of antennas and also explore robust measures to be adaptable to practical systems.

References

[1] S. Ramprashad, G. Caire, and H. Papadopoulos, "Cellular and network MIMO architectures: MU-MIMO spectral efficiency and costs of channel state information," in *IEEE Asilomar Conference on Signals, Systems and Computers*, November 2009, pp. 1811–1818.

[2] G. Caire, N. Jindal, M. Kobayashi, and N. Ravindran, "Multiuser MIMO achievable rates with downlink training and channel state feedback," *IEEE Transactions on Information Theory*, vol. 56, no. 6, pp. 2845–2866, June 2010.

[3] Y. J. Hong, S. M. Kim, and D. K. Sung, "Adaptive random beamforming with interference suppression and beam selection in cellular networks," in *IEEE Global Communications Conference (GLOBECOM)*, Hawaii, USA, November 2009.

[4] D. Gesbert, S. Hanly, H. Huang, S. S. Shitz, O. Simeone, and W. Yu, "Multi-cell MIMO cooperative networks: a new look at interference," *IEEE Journal on Selected Areas in Communications*, vol. 28, no. 9, pp. 1380–1408, December 2010.

[5] G. Caire, S. Ramprashad, H. Papadopoulos, C. Pepin, and C.-E. Sundberg, "Multiuser MIMO downlink with limited inter-cell cooperation: Approximate interference alignment in time, frequency and space," in *46th Annual Allerton Conference on Communication, Control, and Computing*, Allerton House, UIUC, Illinois, USA, September 2008.

[6] S. Jing, D. N. C. Tse, J. Hou, J. B. Soriaga, J. E. Smee, and R. Padovani, "Multi-cell downlink capacity with coordinated processing," in *The Information Theory and Applications Workshop*, San Diego, USA, February 2007.

[7] "Future wireless broadband networks: challenges and possibilities," IEEE C802.16-10/0009, January 2010.

[8] "Physical layer aspects for evolved universal terrestrial radio access," October 2007.

[9] "Evaluation methodology document (emd)," IEEE 802.16m-08/0004r2, July 2008.

[10] C. Suh and D. Tse, "Interference alignment for cellular networks," in *46th Annual Allerton Conference*, Illilois, USA, September 2008, pp. 1037–1044.

[11] B. Zhuang, R. A. Berry, and M. L. Honig, "Interference alignment in MIMO cellular networks," in *IEEE International Conference on Acoustics, Speech, and Signal Processing (ICASSP)*, Prague, Czech Republic, May 2011.

[12] L. Ruan and V. K. Lau, "Interference alignment algorithm for quasi-static MIMO cellular system," in *IEEE Global Communications Conference (GLOBECOM)*, Houston, TX, USA, December 2011.

[13] J. Schreck and G. Wunder, "Iterative interference alignment for cellular systems," in *International ITG Workshop on Smart Antennas (WSA)*, Aachen, February 2011.

[14] C. Suh, M. Ho, and D. N. C. Tse, "Downlink interference alignment," *IEEE Transactions on Communications*, vol. 59, no. 9, pp. 2616–2626, September 2011.

[15] A. Mobasher, A. Bayesteh, and Y. Jia, "Mixed-rank compound MIMO-X interference alignment for multi-user systems," in *IEEE Global Communications Conference (GLOBECOM)*, Houston, TX, USA, December 2011.

[16] A. Bayesteh, A. Mobasher, and Y. Jia, "Downlink multi-user interference alignment in two-cell scenario," in *12th Canadian Workshop on Information Theory (CWIT)*, Kelowna, BC, Canada, May 2011, pp. 182 – 185.

[17] A. Mobasher, A. Bayesteh, and Y. Jia, "Downlink multi-user interference alignment in compound MIMO-X channels," in *12th Canadian Workshop on Information Theory (CWIT)*, Kelowna, BC, Canada, May 2011.

[18] W. Shin, N. Lee, J.-B. Lim, C. Shin, and K. Jang, "On the design of interference alignment scheme for two-cell MIMO interfering broadcast channels," *IEEE Transactions on Wireless Communications*, vol. 10, no. 2, pp. 437–442, February 2011.

[19] S. H. Park and I. Lee, "Degrees of freedom and sum rate maximization for two mutually interfering broadcast channels," in *IEEE International Conference on Communications (ICC)*, Dresden, Germany, June 2009.

[20] J. Kim, S. H. Park, H. Sung, and I. Lee, "Sum rate analysis of two-cell MIMO broadcast channels: spatial multiplexing gain," in *IEEE International Conference on Communications (ICC)*, Cape Town, South Africa, May 2010.

[21] V. Cadambe and S. Jafar, "Interference alignment and degrees of freedom of the K-user interference channel," *IEEE Transactions on Information Theory*, vol. 54, no. 8, pp. 3425–3441, Aug. 2008.

[22] N. Lee, D. Park, and Y. D. Kim, "Degrees of freedom on the K-user MIMO interference channel with constant channel coefficients for downlink communications," in *IEEE Global Communications Conference (GLOBECOM)*, Hawaii, USA, November 2009.

[23] B. Xie, Y. Li, H. Minn, and A. Nosratinia, "Interference alignment under training and feedback constraints," in *IEEE Global Communications Conference (GLOBECOM)*, Houston, TX, USA, December 2011.

[24] A. D. Wyner, "Shannon-theoretic approach to a Gaussian cellular multi-access channel," *IEEE Transactions on Information Theory*, vol. 40, no. 6, pp. 1713–1727, November 1994.

[25] Y. Liu and E. Erkip, "On the sum capacity of K-user cascade Gaussian Z-interference channel," in *IEEE International Symposium on Information Theory*, St. Petersburg, Russia, August 2011, pp. 1382–1386.

[26] J. H. Lee and W. Choi, "Interference alignment by opportunistic user selection in 3-user MIMO interference channels," in *IEEE International Conference on Communications (ICC)*, Kyoto, Japan, June 2011.

[27] ——, "Opportunistic interference alignment by receiver selection in a K-user 1x3 SIMO interference channel," in *IEEE Global Communications Conference (GLOBECOM)*, Houston, TX, USA, December 2011.

[28] ——, "Opportunistic interference aligned user selection in multiuser MIMO interference channels," in *IEEE Global Communications Conference (GLOBECOM)*, Miami, Florida, USA, December 2010.

[29] O. Somekh, O. Simeone, A. Sanderovich, B. M. Zaidel, and S. S. (Shitz), "On the impact of limited-capacity backhaul and inter-users links in cooperative multicell networks," in *42nd Annual Conference on Information Sciences and Systems (CISS)*, Princeton, NJ, July 2008, pp. 776–780.

[30] R. Tandon and H. V. Poor, "On the symmetric feedback capacity of the K-user cyclic interference channel," in *Forty-Ninth Annual Allerton Conference*, Allerton House, UIUC, Illinois, USA, September 2011, pp. 855–862.

[31] L. Zhou and W. Yu, "On the capacity of the K-user cyclic Gaussian interference channel," in *IEEE International Symposium on Information Theory*, St. Petersburg, Russia, August 2011, pp. 1171–1175.
[32] J. S. Kim, S. H. Moon, S. R. Lee, and I. Lee, "A new channel quantization strategy for MIMO interference alignment with limited feedback," *IEEE Transactions on Wireless Communications*, November 2011.
[33] R. T. Krishnamachari and M. K. Varanasi, "Interference alignment under limited feedback for MIMO interference channels," in *IEEE International Symposium on Information Theory (ISIT)*, Austin, Texas, USA, June 2010, pp. 619–623.
[34] M. T. Heath, *Scientific computing: An introductory survey*, 2nd ed. McGraw-Hill, 2002.
[35] G. H. Golub and C. F. V. Loan, *Matrix Computations*, 3rd ed. Johns Hopkins University Press, 1996.
[36] Y. Liang and A. Goldsmith, "Symmetric rate capacity of cellular systems with cooperative base stations," in *IEEE Global Telecommunications Conference (GLOBECOM)*, San Francisco, USA, November 2006.
[37] H. Sung, S.-H. Park, K.-J. Lee, and I. Lee, "Linear precoder desings for K-user interference channels," *IEEE Transactions on Wireless Communications*, vol. 9, no. 1, pp. 291–301, January 2010.
[38] U. Jang, K. Y. Lee, K. S. Cho, and W. Ryu, "Transmit beamforming based inter-cell interference alignment and user selection with CoMP," in *IEEE Vehicular Technology Conference Fall (VTC)*, Ottawa, ON, September 2010.
[39] K. Gomadam, V. Cadambe, and S. Jafar, "Approaching the capacity of wireless networks through distributed interference alignment," in *IEEE Global Telecommunications Conference*, 30 2008-Dec. 4 2008, pp. 1–6.